**A**



**B**

**C**

Fig. 5. IgE-mediated CysLT export from bone marrow-derived mast cells (BMMCs). BMMCs from $mrp1^{-/-}$ and $mrp1^{+/+}$ mice were cultured and stimulated with trinitrophenyl (TNP)-IgE and anti-IgE antibody. Degranulation of BMMCs was assessed using the β-hexosaminidase release assay (A). The amounts of released CysLTs in the culture supernatant (B) and the intracellular contents of CysLTs (C) were measured using ELISA. Data are means ± SD of triplicate samples. *$P < 0.05$; **$P < 0.01$. Results are representative of 3 independent experiments that had similar results.

and IL-13 levels in BALF in OVA-exposed mice and attenuated airway inflammation (14). These previous findings provide direct evidence that CysLTs are involved in the regulation of Th2 immune response-dependent pulmonary inflammation. Our current findings in $mrp1^{-/-}$ mice are consistent with these prior reports, because MRP1 is involved in IgE-mediated LTC4 export from mast cells, and a lack of MRP1 resulted in the decrease of CysLT, antigen-specific IgE, IL-4, and IL-13 levels in the lungs of $mrp1^{-/-}$ mice. Impaired Th2 cytokine production due to MRP1 deficiency might be an important mechanism of reducing airway inflammation in our murine model.

Dendritic cells (DCs) are the most potent antigen presenting cells in the airways and initiate immune responses by presenting antigens to T cells (22). Previous studies have demonstrated that DCs express MRP1, and MRP1 regulates the migration of DCs by transporting LTC4, which promotes chemotaxis to the CCL19 (25). In a model of contact hyper-

sensitivity induced by topical application of FITC, DC migration was substantially attenuated in $mrp1^{-/-}$ mice compared with that observed in $mrp1^{+/+}$ mice (25). In addition, MRP1 transporter activity is also crucial for DC differentiation (27). These aforementioned observations on DCs may contribute to the decreased inflammatory response following OVA exposure that we examined in the lungs of $mrp1^{-/-}$ mice.

MRP1 was the first identified ATP-dependent export pump for LTC4. However, the members of the MRP subfamily, including MRP1–6 and MRP10–12, also mediate the ATP-dependent efflux of organic anions, including glutathione conjugates such as LTC4, across the plasma membrane into the extracellular space (7). We questioned whether the lack of MRP1 in mice would be compensated for by induction or altered expression of other ATP-binding cassette transporter subfamily members. However, van der Deen et al. (30) examined immunohistochemical expression of other transporters such as MRP2, -3, -4, -5, -6, and -9 and breast cancer resistance protein (Brcp) in murine lung tissues and observed no differences in expression of all these transporters in MRP1/MDR1a/1b-deficient mice compared with wild-type mice (30). MRP2, also named the canalicular multispecific organic anion transporter (cMOAT), and MRP1 share very similar substrates, including LTC4 (19). However, Wijnholds et al. (31) demonstrated that anti-cMOAT monoclonal antibody does not detect cMOAT protein on the mast cells in $mrp1^{-/-}$ and $mrp1^{+/+}$ mice, whereas cMOAT in the liver and kidney is readily visualized, and the same holds in $mrp1^{-/-}$ and $mrp1^{+/+}$ tissues. These previous findings strongly suggest that MRP1 (and/or MDR1) deficiency does not affect expression of other transporters in lung tissues in mice and supports our conclusion that inhibition of MRP1 might be a major cause of the impaired development of allergic airway inflammation in the lungs of $mrp1^{-/-}$ mice.

Recent studies have demonstrated that MRP4 can transport leukotrienes (LTB4 and LTC4) and contribute to the migration of DCs, like MRP1 (24) (28). Furthermore, MRP4 is expressed in the bronchial epithelial cells in the lungs (29). These previous findings indicate the possibility that other transporters, such as MRP4, also may be important in the lungs of murine allergic airway inflammation model in addition to MRP1, although expression of other ATP-binding cassette transporters was not altered in the lungs of MRP1-deficient mice. This may be the reason why the differences in the degree of airway inflammation between $mrp1^{-/-}$ and $mrp1^{+/+}$ mice were smaller than expected.

In this study, we also investigated the immunohistochemical expression of MRP1 in the lungs of patients with asthma and in a murine allergic airway inflammation model. MRP1 staining was observed in the cytoplasm and on the plasma membrane of the mast cells, and its expression was also found on macrophages, eosinophils, and bronchial epithelial cells (data not shown). These findings were consistent with prior reports (10), and these cells contain the 5-LO/FLAP/LTC4S pathway and generate LTC4 (16, 23). Among them, the mast cell is the most potent IgE-mediated LTC4-synthesizing cell in allergic airway inflammation and expresses MRP1 in human and murine allergic airway disease. However, eosinophils, macrophages, and bronchial epithelial cells are also important sources of CysLTs. We would like to perform in vitro experiments for CysLT export from eosinophils, macrophages, and

476

bronchial epithelial cells of $mrp1^{-/-}$ mice in a future project. In this study, we focused on the involvement of MRP1 in IgE-dependent CysLT export from mast cells and confirmed that MRP1 plays an important role in the IgE-dependent release of CysLTs from mast cells by using murine BMMCs from $mrp1^{-/-}$ mice. However, decreases in CysLT levels in BALF from $mrp1^{-/-}$ mice in vivo were <50% compared with those in $mrp1^{+/+}$ mice, although the difference was statistically significant ($P = 0.0082$). We speculate that residual CysLT production in $mrp1^{-/-}$ mice may be due to another export pump and/or derived from eosinophils, macrophages, and bronchial epithelial cells. However, it is thought that MRP1 is at least one of the important transporters on mast cells for LTC4 export in the pathogenesis of allergic airway inflammation, although other transporters may exist, because differences in data between $mrp1^{-/-}$ and $mrp1^{+/+}$ mice were statistically significant.

There are a few interesting reports of studies that investigated the association between MRP1 and anti-asthma drugs for patients with bronchial asthma. Bandi et al. (1) incubated the human airway epithelial cell line Calu-1 with budesonide, an anti-asthma corticosteroid, and revealed that treatment with budesonide significantly inhibits MRP1 expression and activity in Calu-1 cells. MRP1 has been screened for genetic variations, and several mutations have been identified in the MRP1 gene in the human population (21). Montelukast is a selective $CysLT_1$ receptor antagonist that is clinically used as an anti-asthma drug. Interestingly, genetic variations in MRP1 are associated with variability in montelukast response in patients with asthma (21). These previous studies suggest that MRP1 polymorphism may be useful as a predictive marker for the efficacy of therapy in the management of asthma.

In conclusion, our study revealed that airway inflammation and goblet cell hyperplasia after OVA exposure were reduced in $mrp1^{-/-}$ mice compared with $mrp1^{+/+}$ mice. Levels of CysLTs, antigen-specific IgE, IL-4, and IL-13 in BALF from OVA-exposed $mrp1^{-/-}$ mice were significantly lower than those from OVA-exposed $mrp1^{+/+}$ mice. Export of IgE-dependent CysLTs from murine BMMCs was mediated by MRP1. On the basis of these findings, MRP1 expressed on mast cells functions as a CysLT export pump in the development of allergic airway disease. These findings also suggest the possibility that MRP1 may be one of the important therapeutic targets and provide new insights for understanding its role in allergic asthma.

## REFERENCES

1. Bandi N, Kompella UB. Budesonide reduces multidrug resistance-associated protein 1 expression in an airway epithelial cell line (Calu-1). *Eur J Pharmacol* 437: 9–17, 2002.
2. Bartosz G, Konig J, Keppler D, Hagmann W. Human mast cells secreting leukotriene C4 express the MRP1 gene-encoded conjugate export pump. *Biol Chem* 379: 1121–1126, 1998.
3. Borst P, Evers R, Kool M, Wijnholds J. A family of drug transporters: the multidrug resistance-associated proteins. *J Natl Cancer Inst* 92: 1295–1302, 2000.
4. Busse WW, Lemanske RF Jr. Asthma. *N Engl J Med* 344: 350–362, 2001.
5. Campbell BJ, Baker SF, Shukla SD, Forrester LJ, Zahler WL. Bioconversion of leukotriene D4 by lung dipeptidase. *Biochim Biophys Acta* 1042: 107–112, 1990.
6. Cole SP, Bhardwaj G, Gerlach JH, Mackie JE, Grant CE, Almquist KC, Stewart AJ, Kurz EU, Duncan AM, Deeley RG. Overexpression of a transporter gene in a multidrug-resistant human lung cancer cell line. *Science* 258: 1650–1654, 1992.
7. Deeley RG, Westlake C, Cole SP. Transmembrane transport of endo- and xenobiotics by mammalian ATP-binding cassette multidrug resistance proteins. *Physiol Rev* 86: 849–899, 2006.
8. Drazen JM, Israel E, O'Byrne PM. Treatment of asthma with drugs modifying the leukotriene pathway. *N Engl J Med* 340: 197–206, 1999.
9. Duan W, Chan JH, Wong CH, Leung BP, Wong WS. Anti-inflammatory effects of mitogen-activated protein kinase kinase inhibitor U0126 in an asthma mouse model. *J Immunol* 172: 7053–7059, 2004.
10. Flens MJ, Zaman GJ, van der Valk P, Izquierdo MA, Schroeijers AB, Scheffer GL, van der Groep P, de Haas M, Meijer CJ, Scheper RJ. Tissue distribution of the multidrug resistance protein. *Am J Pathol* 148: 1237–1247, 1996.
11. Gondokaryono SP, Ushio H, Niyonsaba F, Hara M, Takenaka H, Jayawardana ST, Ikeda S, Okumura K, Ogawa H. The extra domain A of fibronectin stimulates murine mast cells via Toll-like receptor 4. *J Leukoc Biol* 82: 657–665, 2007.
12. Henderson WR Jr. The role of leukotrienes in inflammation. *Ann Intern Med* 121: 684–697, 1994.
13. Henderson WR Jr, Lewis DB, Albert RK, Zhang Y, Lamm WJ, Chiang GK, Jones F, Eriksen P, Tien YT, Jonas M, Chi EY. The importance of leukotrienes in airway inflammation in a mouse model of asthma. *J Exp Med* 184: 1483–1494, 1996.
14. Henderson WR Jr, Tang LO, Chu SJ, Tsao SM, Chiang GK, Jones F, Jonas M, Pae C, Wang H, Chi EY. A role for cysteinyl leukotrienes in airway remodeling in a mouse asthma model. *Am J Respir Crit Care Med* 165: 108–116, 2002.
15. Hipfner DR, Deeley RG, Cole SP. Structural, mechanistic and clinical aspects of MRP1. *Biochim Biophys Acta* 1461: 359–376, 1999.
16. Jame AJ, Lackie PM, Cazaly AM, Sayers I, Penrose JF, Holgate ST, Sampson AP. Human bronchial epithelial cells express an active and inducible biosynthetic pathway for leukotrienes B4 and C4. *Clin Exp Allergy* 37: 880–892, 2007.
17. Kanaoka Y, Boyce JA. Cysteinyl leukotrienes and their receptors: cellular distribution and function in immune and inflammatory responses. *J Immunol* 173: 1503–1510, 2004.
18. Kim DC, Hsu FI, Barrett NA, Friend DS, Grenningloh R, Ho IC, Al-Garawi A, Lora JM, Lam BK, Austen KF, Kanaoka Y. Cysteinyl leukotrienes regulate Th2 cell-dependent pulmonary inflammation. *J Immunol* 176: 4440–4448, 2006.
19. Leier I, Jedlitschky G, Buchholz U, Cole SP, Deeley RG, Keppler D. The MRP gene encodes an ATP-dependent export pump for leukotriene C4 and structurally related conjugates. *J Biol Chem* 269: 27807–27810, 1994.
20. Leier I, Jedlitschky G, Buchler M, Buchholz U, Bron M, Keppler D. Identification of the biosynthetic leukotriene C4 export pump in murine mastocytoma cells as a homolog of the multidrug-resistance protein. *Eur J Biochem* 242: 201–205, 1996.
21. Lima JJ, Zhang S, Grant A, Shao L, Tantisira KG, Allayee H, Wang J, Sylvester J, Holbrook J, Wise R, Weiss ST, Barnes K. Influence of leukotriene pathway polymorphisms on response to montelukast in asthma. *Am J Respir Crit Care Med* 173: 379–385, 2006.
22. Machida I, Matsuse H, Kondo Y, Kawano T, Saeki S, Tomari S, Obase Y, Fukushima C, Kohno S. Cysteinyl leukotrienes regulate dendritic cell functions in a murine model of asthma. *J Immunol* 172: 1833–1838, 2004.
23. Penrose JF, Austen KF. The biochemical, molecular, and genomic aspects of leukotriene C4 synthase. *Proc Assoc Am Physicians* 111: 537–546, 1999.
24. Rius M, Hummel-Eisenbeiss J, Keppler D. ATP-dependent transport of leukotrienes B4 and C4 by the multidrug resistance protein ABCC4 (MRP4). *J Pharmacol Exp Ther* 324: 86–94, 2008.
25. Robbiani DF, Finch RA, Jager D, Muller WA, Sartorelli AC, Randolph GJ. The leukotriene C(4) transporter MRP1 regulates CCL19 (MIP-3beta,

ELC)-dependent mobilization of dendritic cells to lymph nodes. *Cell* 103: 757–768, 2000.

26. **Supajatura V, Ushio H, Nakao A, Okumura K, Ra C, Ogawa H.** Protective roles of mast cells against enterobacterial infection are mediated by Toll-like receptor 4. *J Immunol* 167: 2250–2256, 2001.

27. **Van de Ven R, de Jong MC, Reurs AW, Schoonderwoerd AJ, Jansen G, Hooijberg JH, Scheffer GL, de Gruijl TD, Scheper RJ.** Dendritic cells require multidrug resistance protein 1 (ABCC1) transporter activity for differentiation. *J Immunol* 176: 5191–5198, 2006.

28. **Van de Ven R, Scheffer GL, Reurs AW, Lindenberg JJ, Oerlemans R, Jansen G, Gillet JP, Glasgow JN, Pereboev A, Curiel DT, Scheper RJ, de Gruijl TD.** A role for multidrug resistance protein 4 (MRP4; ABCC4) in human dendritic cell migration. *Blood* 112: 2353–2359, 2008.

29. **Van der Deen M, de Vries EG, Timens W, Scheper RJ, Timmer-Bosscha H, Postma DS.** ATP-binding cassette (ABC) transporters in normal and pathological lung. *Respir Res* 6: 59, 2005.

30. **Van der Deen M, Timens W, Timmer-Bosscha H, van der Strate BW, Scheper RJ, Postma DS, de Vries EG, Kerstjens HA.** Reduced inflammatory response in cigarette smoke exposed Mrp1/Mdr1a/1b deficient mice. *Respir Res* 8: 49, 2007.

31. **Wijnholds J, Evers R, van Leusden MR, Mol CA, Zaman GJ, Mayer U, Beijnen JH, van der Valk M, Krimpenfort P, Borst P.** Increased sensitivity to anticancer drugs and decreased inflammatory response in mice lacking the multidrug resistance-associated protein. *Nat Med* 3: 1275–1279, 1997.

nature
medicine

# *RPN2* gene confers docetaxel resistance in breast cancer

Kimi Honma[1,2], Kyoko Iwao-Koizumi[3], Fumitaka Takeshita[1], Yusuke Yamamoto[1], Teruhiko Yoshida[4], Kazuto Nishio[5], Shunji Nagahara[6], Kikuya Kato[3] & Takahiro Ochiya[1]

Drug resistance acquired by cancer cells has led to treatment failure. To understand the regulatory network underlying docetaxel resistance in breast cancer cells and to identify molecular targets for therapy, we tested small interfering RNAs (siRNAs) against 36 genes whose expression was elevated in human nonresponders to docetaxel for the ability to promote apoptosis of docetaxel-resistant human breast cancer cells (MCF7-ADR cells). The results indicate that the downregulation of the gene encoding ribophorin II (RPN2), which is part of an *N*-oligosaccharyl transferase complex, most efficiently induces apoptosis of MCF7-ADR cells in the presence of docetaxel. RPN2 silencing induced reduced glycosylation of the P-glycoprotein, as well as decreased membrane localization, thereby sensitizing MCF7-ADR cells to docetaxel. Moreover, *in vivo* delivery of siRNA specific for *RPN2* markedly reduced tumor growth in two types of models for drug resistance. Thus, RPN2 silencing makes cancer cells hypersensitive response to docetaxel, and RPN2 might be a new target for RNA interference–based therapeutics against drug resistance.

Breast cancer is the most common malignancy in women. Either neoadjuvant or adjuvant chemotherapy administered to subjects with stage 1–3 breast cancers can improve their survival rates[1–3]. Among chemotherapeutic agents, docetaxel, which belongs to the group of taxanes (mitotic inhibitors and antimicrotubule agents), has been shown to have well-established benefits in breast cancer[4]. The response rate to docetaxel, however, is 50% even in first-line chemotherapy, and it decreases to 20–30% in second- or third-line chemotherapy[5–7]; nearly half of the treated subjects do not respond to it and suffer side effects. There is currently no method to reliably predict tumor responses to docetaxel before therapy or to detect when resistance or hypersensitivity develops. Therefore, the identification of molecular biomarkers in docetaxel-resistant breast cancer that could help in a more accurate assessment of individual treatment and the development of molecular-target therapies that could lead to better tumor reduction are of considerable interest.

It has been reported that the expression of the multidrug transporter P-glycoprotein, encoded by the *MDR1* gene (official gene symbol *ABCB1*), is one of the causes of clinical drug resistance to taxanes[8,9]. Other molecules, such as the multidrug resistance–associated protein MRP1[10,11], breast cancer resistance protein (*ABCG2*) and other transporters[12], which act as energy-dependent efflux pumps capable of expelling a large range of xenobiotics, and GSTpi, which is one of the isoenzymes of the glutathione-*S*-transferase (GST)[13–15], have been extensively reported to be overexpressed in tumor cells showing the multidrug-resistant phenotype. It was recently shown that high thioredoxin expression is associated with resistance to docetaxel in breast cancer[16,17]. These molecules might be clinically useful in the prediction of a response to anticancer drugs. Currently, however, none have proven to be specific target molecules for increasing the efficacy of chemotherapy in breast cancer.

To better understand the regulatory network underlying docetaxel resistance in breast cancer cells and to identify molecular targets for therapy, we initiated gene expression profiling of 44 subjects with breast tumors (22 responders and 22 nonresponders) by adaptor-tagged competitive PCR[18] to identify the genes capable of predicting a docetaxel response in human breast cancer and reported the preliminary results of 85 genes whose expression potentially correlated with docetaxel resistance[16]. In the current study, we used an atelocollagen-based siRNA cell transfection array[19,20] to identify the genes responsible for conferring drug resistance. Among the siRNAs targeting genes that were elevated in nonresponders to docetaxel, siRNA designed for *RPN2* (RNP2 siRNA) significantly promoted docetaxel-dependent apoptosis and cell growth inhibition of MCF7-ADR human breast cancer cells that are resistant to docetaxel. Furthermore, atelocollagen-mediated *in vivo* delivery of RPN2 siRNA significantly reduced drug-resistant tumor growth in mice given docetaxel. RPN2 confers drug resistance via the glycosylation of P-glycoproteins and regulates antiapoptotic genes. Thus, RPN2 siRNA introduction hypersensitizes cancer cell response to chemotherapeutic agents, making RPN2 a potential key target for future RNA interference (RNAi)-based therapeutics against a drug-resistant tumor.

[1]Section for Studies on Metastasis, Japanese National Cancer Center Research Institute, 1-1, Tsukiji, 5-chome, Chuo-ku, Tokyo 104-0045, Japan. [2]Koken Bioscience Institute, KOKEN, 2-13-10 Ukima, Kita-ku, Tokyo 115-0051, Japan. [3]Research Institute, Osaka Medical Center for Cancer and Cardiovascular Diseases, 1-3-2 Nakamichi, Higashinari-ku, Osaka 537-8511, Japan. [4]Genetics Division and [5]Pharmaceutical Division, Japanese National Cancer Center Research Institute, 1-1, Tsukiji, 5-chome, Chuo-ku, Tokyo 104-0045, Japan. [6]Dainippon Sumitomo Pharma, 3-45, Kurakakiuchi, 1-chome, Ibaraki, Osaka 567-0878, Japan. Correspondence should be addressed to T.O. (tochiya@ncc.go.jp).

## RESULTS

### RNAi-based screening for identification of molecular target

As an extension of our previous strategy of analyzing docetaxel resistance in breast cancer cells and of identifying molecular targets for therapy[16], we conducted a study of RNAi-induced gene knockdown in docetaxel-resistant MCF7-ADR human breast cancer cells. Among the 85 genes listed[16], 61 genes that are potentially targets for siRNA strategy were upregulated in human nonresponders. We selected 36 genes with more than a 0.365 signal-to-noise ratio and successfully designed and synthesized siRNAs specific to these genes (**Table 1**). The siRNAs were conjugated to atelocollagen and arrayed on a 96-well microplate. Then, MCF7-ADR cells expressing the luciferase gene (MCF7-ADR-Luc) were seeded into the microplate (the target validation process by cell transfection array is schematically shown in **Supplementary Fig. 1** online.). To evaluate the efficiency of the atelocollagen-mediated cell transfection array, we used GL3 siRNA against the gene encoding luciferase. Atelocollagen-mediated GL3 siRNA delivery caused an approximate 75% reduction of the luciferase activity in MCF7-ADR-Luc cells relative to the control nontargeting siRNA (data not shown). To identify the genes responsible for docetaxel resistance, we assessed siRNAs for their ability to inhibit

cell growth and induce apoptosis in the presence of docetaxel compared with the control nontargeting siRNA. We measured cell growth by luciferase activity and examined apoptosis by caspase-7 activation. The results indicated that the downregulation of eight genes (*PTPLB, GSTP1, TUBB, RPN2, SQRDL, NDUFS3, PDCD5* and *MRPL17*) resulted in marked inhibition of cell growth ($P < 0.05$, **Fig. 1a**). Induction of apoptosis was evidenced in cells by downregulation of six genes (*PTPLB, APRT, CFL1, RPN2, SQRDL* and *MRPL17*; $P < 0.05$, **Fig. 1b**). In particular, RPN2 siRNA strongly enhanced caspase-7 activity in the presence of docetaxel ($P < 0.001$, **Supplementary Fig. 2a** online). We validated these results by counting Hoechst-stained cells showing apoptotic nuclear condensation and fragmentation (**Fig. 2a**) and found that there was a significantly higher apoptotic cell death rate in cells given RPN2 siRNA and docetaxel relative to that in cells given RPN2 siRNA alone ($P < 0.02$, **Fig. 2b**). No significant difference was observed in cells with nontargeting control siRNA (**Fig. 2b**). At 72 h after treatment with siRNA and docetaxel, there was substantial cell death induced by RPN2 siRNA compared with the control nontargeting siRNA (**Fig. 2c**). At 96 h after the transfection, almost all RPN2 siRNA–treated cells were detached and disappeared from the culture dishes.

**Table 1 The list of 36 genes whose expression is elevated in nonresponders to docetaxel in subjects with breast cancer**

| No | Gene | Description | Accession number |
|---|---|---|---|
| 1 | UFM1 | Ubiquitin-fold modifier 1 | BC005193 |
| 2 | PTPLB | Protein tyrosine phosphatase-like (proline instead of catalytic arginine), member b | AF052159 |
| 3 | S100A10 | S100 calcium binding protein A10 | M38591 |
| 4 | APRT | Adenine phosphoribosyltransferase | Y00486 |
| 5 | CFL1 | Cofilin-1 (non-muscle) | X95404 |
| 6 | GSTP1 | Glutathione S-transferase pi 1 | M24485 |
| 7 | HSPA5 | Heat shock 70 kDa protein 5 (glucose-regulated protein, 78 kDa) | M19645 |
| 8 | GNB2L1 | Guanine nucleotide binding protein (G protein), β polypeptide 2 like 1 | M24194 |
| 9 | TUBB | Tubulin, β | BC001002 |
| 10 | MX1 | Myxovirus (influenza virus) resistance 1, interferon-inducible protein p78 (mouse) | M33882 |
| 11 | COX7C | Cytochrome c oxidase subunit VIIc | BC001005 |
| 12 | RPN2 | Ribophorin II | Y00282 |
| 13 | DYNLL1 | Dynein, light chain, LC8-type 1 | U32944 |
| 14 | FXR1 | Fragile X mental retardation, autosomal homolog 1 | U25165 |
| 15 | SQRDL | Sulfide quinone reductase-like (yeast) | AF151802 |
| 16 | NDUFS3 | NADH dehydrogenase (ubiquinone) Fe-S protein 3, 30 kDa (NADH-coenzyme Q reductase) | AL135819 |
| 17 | EST | ESTs | AL358933 |
| 18 | C19orf10 | Chromosome 19 open reading frame 10 | BC003639 |
| 19 | ATP5E | ATP synthase, H+ transporting, mitochondrial F1 complex, ε subunit | AF052955 |
| 20 | PDCD5 | Programmed cell death 5 | AF014955 |
| 21 | CLPTM1L | CLPTM1-like | AL137440 |
| 22 | PPP1R14B | Protein phosphatase 1, regulatory (inhibitor) subunit 14B | X91195 |
| 23 | MRPL17 | Mitochondrial ribosomal protein L17 | AK026857 |
| 24 | TUBA1B | Tubulin, α1b | BC006481 |
| 25 | IFI6 | Interferon, α-inducible protein 6 | X02492 |
| 26 | GAPDH | Glyceraldehyde-3-phosphate dehydrogenase | AF261085 |
| 27 | SLC25A3 | Solute carrier family 25 (mitochondrial carrier; phosphate carrier), member 3 | BC006455 |
| 28 | MAD2L2 | MAD2 mitotic arrest deficient-like 2 (yeast) | AF157482 |
| 29 | CTNNB1 | Catenin (cadherin-associated protein), β1, 88 kDa | X87838 |
| 30 | CALR | Calreticulin | M84739 |
| 31 | MRPS6 | Mitochondrial ribosomal protein S6 | BC000547 |
| 32 | ANGPTL2 | Angiopoietin-like 2 | AF007150 |
| 33 | RPL38 | Ribosomal protein L38 | Z26876 |
| 34 | ANAPC7 | Anaphase promoting complex subunit 7 | AY007104 |
| 35 | ENO1 | Enolase 1, (α) | BC004325 |
| 36 | ALDH2 | Aldehyde dehydrogenase 2 family (mitochondrial) | M20456 |
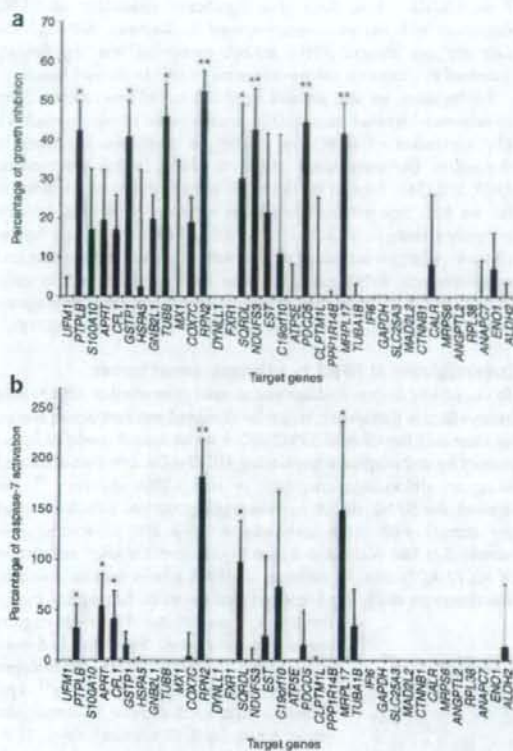
**Figure 1** RNAi cell transfection array analysis in cultured breast cancer cells. (a) Inhibition of cell growth by 36 siRNAs on atelocollagen-based cell transfection arrays in the presence of docetaxel (1 nM) 72 h after transfection. The cell growth was estimated by luciferase activity in MCF7-ADR-Luc cells, which stably express luciferase ($n$ = 4 per group; $*P < 0.05$, $**P < 0.01$). (b) Activation of caspase-7 by 36 siRNAs on atelocollagen-based cell transfection arrays in the presence of docetaxel (1 nM) 72 h after transfection. After the detection of luciferase activity, the same cell transfection arrays were assigned to the measurement of caspase-7 activity, which is elevated in apoptotic MCF7-ADR-Luc cells ($n$ = 4 per group; $*P < 0.05$, $**P < 0.01$). Values are means ± s.d.

In addition, we established stable clones expressing short hairpin RNA (shRNA) against RPN2 (shRNP2) and examined the effect on apoptosis induction in MCF7-ADR cells. The clone that expressed the lowest RPN2 mRNA level showed a 70% reduction of RPN2 expression relative to the control clone ($P < 0.001$, Supplementary Fig. 2c), and this shRPN2 clone showed a high caspase-7 activity as compared to the control clone in the presence of docetaxel ($P < 0.001$, Supplementary Fig. 2d). We examined seven independent clones and found that they all showed a similar phenotype of increasing drug sensitivity (data not shown). Therefore, consistent with our results with synthetic RPN2 siRNA, the data from the shRPN2 experiments provide evidence for the involvement of RPN2 in drug resistance.

To evaluate the effect of RPN2 siRNA on the drug response of MCF7-ADR cells, we measured the half-maximal inhibitory concentration ($IC_{50}$) for taxanes. The $IC_{50}$ values for docetaxel in MCF7 and MCF7-ADR cells were 9.48 ± 1.48 nM and 40.22 ± 5.14 nM, respectively ($P < 0.001$). RPN2 siRNA–transfected MCF7-ADR cells were 3.5-fold more sensitive to docetaxel compared with nontargeting siRNA–transfected cells ($IC_{50}$ of 11.47 ± 1.97 nM versus 39.48 ± 2.98 nM, $P < 0.001$). Thus, RPN2 silencing makes MCF7-ADR cells sensitive to docetaxel to a degree similar to that in drug-sensitive MCF7 cells. For paclitaxel, another taxane, the $IC_{50}$ values in MCF7 and MCF7-ADR cells were 13.00 ± 2.02 nM and 89.74 ± 3.43 nM, respectively ($P < 0.001$). RPN2 siRNA–transfected MCF7-ADR cells were 2.6-fold more sensitive to paclitaxel compared with nontargeting siRNA–transfected cells ($IC_{50}$ of 32.92 ± 3.89 nM versus 84.39 ± 5.48 nM, $P < 0.001$). These results indicate that RPN2 silencing bestows a hypersensitive response to taxanes to drug-resistant breast cancer cells.

In addition, we examined docetaxel-resistant EMT6/AR10.0 cells with high expression of the mouse Rpn2 gene and the Mdr1 (Abcb1b) and Mdr3 (Abcb1a) genes, which reportedly have a similar role in drug resistance to that of the MDR1 gene in humans, to see whether they have a similar phenotype to MCF7-ADR cells in terms of RPN2 expression status and drug resistance. The siRNA-mediated knockdown of mouse Rpn2 (70% reduction of mRNA by real-time RT-PCR analysis) significantly induced apoptosis of cells in the presence of docetaxel (Supplementary Fig. 2e–g). In contrast, nontargeting control siRNA showed no effect (Supplementary Fig. 2e–g). Therefore, these results suggest that RPN2 confers docetaxel resistance to both human and mouse cell lines.

However, the expression of other genes was also found to correlate with docetaxel resistance by RNAi-based screening, and they could have some possible additive or synergistic effects with RPN2. Thus, we examined the induction of apoptosis after cotransfection of RPN2 siRNA and siRNAs against other genes that caused cell growth inhibition, apoptosis induction or both in docetaxel-resistant MCF7-ADR cells. Knockdown of PTPLB, APRT, CFL1, GSTP1, TUBB, SQRDL, NDUFS3, PDCD5 or MRPL17 genes with simultaneous knockdown of RPN2 did not significantly enhance caspase-7 activity relative to the knockdown of RPN2 alone (Supplementary Fig. 2b). This result shows that knockdown of the other genes does not have an additive effect when used together with knockdown of RPN2.

We confirmed the efficacy of RPN2 siRNA for the knockdown of RPN2 messenger RNA by cell-direct real-time RT-PCR analysis. This analysis revealed that RPN2 siRNA inhibited 80% of the mRNA level relative to the control nontargeting siRNA (Fig. 2d). Immunofluorescence staining of the RPN2 protein revealed that the RPN2 protein localized in the cytoplasm and its expression was decreased by RPN2 siRNA (Fig. 2e). In further experiments, a liposome-mediated RPN2 siRNA transfection was performed. The western blot analysis showed a 45% reduction in RPN2 protein abundance (90% reduction of mRNA by real-time RT-PCR analysis) by RPN2 siRNA transfection in comparison with the control nontargeting siRNA (Fig. 2f). These results suggest that downregulation of RPN2 expression by siRNA inhibits cell growth and induces apoptosis in the presence of docetaxel.

## Induction of RPN2 expression by docetaxel treatment

Real-time RT-PCR analysis showed that docetaxel-resistant MCF7-ADR cells expressed a slightly increased level of RPN2 mRNA (approximately 20%, $P < 0.01$) relative to parental MCF7 cells (Fig. 3a). However, RPN2 mRNA expression in parental MCF7 cells was markedly induced by docetaxel in a dose-dependent manner at

48 h after treatment (**Fig. 3b**). These data indicate that RPN2 mRNA induction may correlate with the observed antiapoptotic phenotype of MCF7-ADR cells.

Furthermore, MCF7-ADR cells expressed abundant MDR1 mRNA, which is a major cause of docetaxel resistance, whereas docetaxel-sensitive MCF7 cells did not (**Fig. 3c**). Additionally, MDR1 mRNA expression in MCF7 cells was strongly induced by docetaxel at 48 h after treatment (**Fig. 3d**). Together, these data provide a new insight into the development of docetaxel resistance in MCF7 cells: when breast cancer cells coordinately express a high amount the of *MDR1* and *RPN2* gene products, the cells become drug-resistant.

### RPN2 expression associates with response to docetaxel

In this study, subjects with breast cancer with complete response and partial response were defined as responders, whereas subjects with no change and progressive disease were defined as nonresponders, in accordance with World Health Organization criteria[16] (**Supplementary Note** online).

Of the 44 subjects, 22 showed a pathologic response to docetaxel, and the other 22 showed no response[16]. To understand the clinical importance of the status of RPN2 expression in the subjects, we compared the expression level (signal log ratio) for RPN2 transcript between nonresponder and responder subjects by the Mann-Whitney U-test. The subjects with higher RPN2 expression showed a significantly lower response rate to docetaxel than did those with relatively low expression of RPN2 (signal log ratio expressed as mean ± s.e.m. in nonresponders was 0.347 ± 0.062 versus 0.111 ± 0.052 in responders;

$P = 0.0052$). Thus, there is a significant association of RPN2 expression with the pathologic response to docetaxel. Although the data are not shown, RPN2 mRNA expression was significantly increased in cancerous tissues compared to that in normal tissues.

Furthermore, we also assessed validated sets of new samples from 26 subjects with breast tumors (12 responders and 14 nonresponders). The expression of RPN2 was higher in nonresponders than in responders (nonresponders, 0.240 ± 0.066, versus responders, 0.025 ± 0.194). Because of the small sample size in the validation set, we have not obtained conclusive results at this time. We are currently seeking larger samples that will be tested in the near future. However, when we combined studies with subjects in the learning and validation sets, RPN2 expression was significantly higher in nonresponders (34 subjects) than in responders (36 subjects) (nonresponders, 0.306 ± 0.046, versus responders, 0.080 ± 0.075; $P = 0.0219$).

### Downregulation of RPN2 in orthotopic breast tumors

To extend our *in vitro* findings and to determine whether RPN2 could be an effective therapeutic target for docetaxel-resistant breast cancer, we examined the effect of RPN2 siRNA on an animal model of breast tumors by orthotopically implanting MCF7-ADR cells into mice and using an atelocollagen-mediated *in vivo* siRNA delivery[21,22]. We injected the RPN2 siRNA or nontargeting control siRNA (1 nmol per tumor) with 0.5% atelocollagen in a 200 μl volume into tumors that had reached 4–5 mm in diameter 7 d after inoculation of MCF7-ADR cells. At the time of siRNA administration, docetaxel was intraperitoneally (i.p.) injected into the mice. Subsequent tumor

development was monitored by measuring the tumor size for a week. Mice that had been administered the RPN2 siRNA–atelocollagen complex and docetaxel (20 mg kg$^{-1}$ i.p.) showed a significant decrease in tumor size (mean ± s.d.; day 0, 52 ± 8 mm$^3$; day 7, 21 ± 8 mm$^3$) relative to mice that had been administered the control nontargeting siRNA–atelocollagen (day 0, 37 ± 7 mm$^3$; day 7, 35 ± 12 mm$^3$; $P < 0.01$) (**Fig. 4a**). The tumor size was markedly reduced by administration of RPN2 siRNA with docetaxel at 7 d after treatment (**Fig. 4b**). In the absence of docetaxel, RPN2 siRNA treatment slightly reduced MCF7-ADR tumor size relative to controls; however, there were no statistically significant differences (**Supplementary Fig. 3a** online). We also observed that docetaxel alone had no significant effect on tumor growth (**Supplementary Fig. 3a**). Furthermore, no significant differences were observed in tumor growth between mice treated with control nontargeting siRNA and untreated mice in the presence or in the absence of docetaxel (data not shown). Thus, RPN2 siRNA is useful for reducing the size of orthotopic MCF7-ADR breast tumors in the presence of docetaxel. Additionally, to evaluate the effect of sustained treatment with siRNA, we treated mice with tumors twice by injection of siRNA-atelocollagen complex. RPN2 siRNA or nontargeting control siRNA (1 nmol per tumor) were injected into the tumors (diameter, 4 mm) at days 0
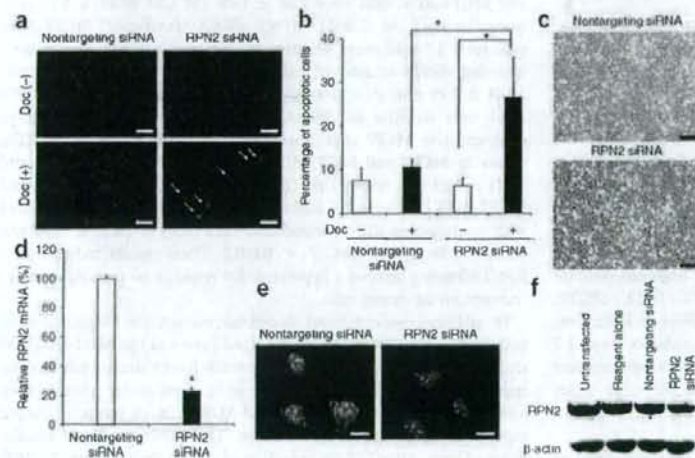
**Figure 2** Apoptosis of MCF7-ADR cells transduced with RPN2 siRNA. (**a**) Hoechst staining of cells in the presence or absence of docetaxel (Doc, 1 nM) 72 h after the transfection of RPN2 siRNA. Scale bar, 50 μm. The arrows indicate cells with nuclear condensation and fragmentation. (**b**) Numbers of apoptotic cells from **a**. The data show the percentage of apoptotic cells in the presence or absence of docetaxel (1 nM) 72 h after the transfection of RPN2 siRNA. As a control, nontargeting control siRNA was used ($n = 4$ per group, *$P < 0.02$). (**c**) Phase-contrast micrograph of MCF7-ADR cells 72 h after treatment with RPN2 siRNAs or control nontargeting siRNAs in the presence of docetaxel. Scale bar, 200 μm. (**d**) Knockdown of RPN2 mRNA by RPN2 siRNA in a cell transfection array, as monitored by cell-direct real-time RT-PCR analysis. As a control, nontargeting siRNA was used ($n = 4$ per group, *$P < 0.001$). (**e**) Immunofluorescence staining of the RPN2 protein in MCF7-ADR cells 72 h after treatment with RPN2 siRNAs or control nontargeting siRNAs. Scale bar, 5 μm. (**f**) Western blot analysis of RPN2 protein in MCF7-ADR cells treated with RPN2 siRNAs or control nontargeting siRNAs 72 h after the liposome-mediated transfection. Values are means ± s.d.
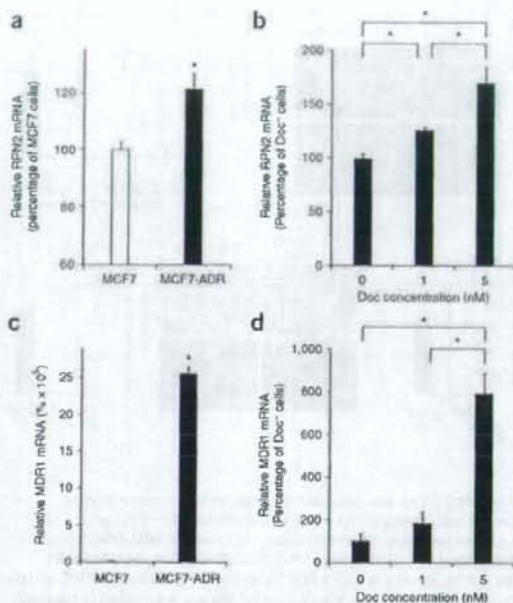
**Figure 3** Induction of RPN2 and MDR1 expression by docetaxel treatment. RPN2 mRNA and MDR1 mRNA expression were analyzed by real-time RT-PCR. (a) RPN2 expression in drug-resistant MCF7-ADR cells and parental drug-sensitive MCF7 cells ($n = 3$ per group, $*P < 0.01$). (b) Expression of RPN2 induced by docetaxel treatment in parental MCF7 cells. The data shown are from 48 h after the treatment ($n = 3$ per group, $*P < 0.01$). (c) MDR1 expression in drug-resistant MCF7-ADR cells and parental drug-sensitive MCF7 cells ($n = 3$ per group, $*P < 0.001$). The numbers on the $y$ axis represent percentage ($\times 10^5$) of MCF7 cells. (d) Expression of MDR1 induced by docetaxel treatment in parental MCF7 cells. The data shown are from 48 h after the treatment ($n = 3$ per group, $*P < 0.01$). Values are means ± s.d.

and 10. Simultaneously, docetaxel (20 mg kg$^{-1}$ i.p.) was injected into the mice. We observed the mice for 20 d. Mice that had been given RPN2 siRNA and docetaxel showed significantly suppressed tumor growth relative to the mice that were administered control nontargeting siRNA at day 20 after the treatment ($P < 0.05$, **Supplementary Fig. 3b,c**). Mice showed no toxic effect during the observation period.

Furthermore, we examined the effect of RPN2 siRNA on a second animal model of breast tumors by orthotopically implanting MDA-MB-231/MDR1 cells. First, we established an MDA-MB-231/MDR1 cell line, which expresses the *MDR1* gene inducing docetaxel resistance. In this study, MDR1 expression is a key factor, because we are proposing that the coordinate expressions of RPN2 and P-glycoprotein may participate in the mechanism of docetaxel resistance. We injected the RPN2 siRNA or nontargeting control siRNA (2 nmol per tumor) with 0.5% atelocollagen in a 200 µl volume into tumors that were 5–6 mm in diameter 8 d after inoculation of MDA-MB-231/MDR1 cells. At the same time of siRNA administration, we injected docetaxel i.p. into the mice. Because docetaxel at a dose of 20 mg kg$^{-1}$ in mice slightly suppressed MDA-MB-231/MDR1 tumor growth, we reduced the dose of docetaxel to 7 mg kg$^{-1}$, corresponding to the IC$_{50}$ value of docetaxel in MDA-MB-231/MDR1 cells, which was 35% of that of MCF7-ADR cells. At a dose of 7 mg kg$^{-1}$ docetaxel, mice treated with docetaxel alone showed no significant change in tumor growth. Subsequent tumor development was monitored by measuring the tumor size for a week. Mice that had been administered the RPN2 siRNA–atelocollagen complex and docetaxel (7 mg kg$^{-1}$ i.p.) showed a significant inhibition of tumor growth (day 0, 61 ± 21 mm$^3$; day 7, 97 ± 24 mm$^3$) relative to mice that had been administered the control nontargeting siRNA–atelocollagen complex (day 0, 68 ± 9 mm$^3$; day 7, 154 ± 23 mm$^3$) (**Fig. 4c,d**). The value was statistically significant, with $P < 0.002$. Tumors treated with RPN2 siRNA in the absence of docetaxel showed no significant inhibition relative to control tumors that had been given nontargeting

siRNA or docetaxel alone (data not shown). These results show that the growth of docetaxel-resistant MDA-MB-231/MDR1 tumors was suppressed by administration of RPN2 siRNA and docetaxel. Thus, RPN2 silencing is effective for the suppression of tumor growth in two models for docetaxel-resistant breast cancer in the presence of docetaxel.

### RPN2 siRNA delivery augments docetaxel-induced apoptosis

MCF7-ADR tumors treated with RPN2 siRNA were investigated for apoptotic activity after docetaxel treatment for 3 d. TUNEL staining of tumor tissue treated with RPN2 siRNA revealed a significant number of apoptotic cells relative to the number in nontargeting control siRNA–treated tumors ($P < 0.01$, **Fig. 4e,f**). In contrast, RPN2 siRNA–transduced tumors in the absence of docetaxel showed no marked apoptotic cell death (**Fig. 4e,f**). We have also previously shown that atelocollagen alone does not induce any cytotoxic or inflammatory effect when it is injected into mice[23,24]. In a subsequent experiment, the mRNA levels of RPN2 in treated tumors were measured. RPN2 expression was significantly reduced in mouse tumors after combined treatment with RPN2 siRNA and docetaxel ($P < 0.05$, **Fig. 4g**). Furthermore, the RPN2 protein abundance in treated tumors was markedly downregulated by RPN2 siRNA (**Fig. 4h**). Thus, these results altogether indicate that RPN2 siRNA induces tumor inhibition via augmentation of docetaxel-induced apoptotic cell death *in vivo*.

To examine docetaxel retention in the tumors in the *in vivo* experiment, we performed drug disposition analysis. Eleven hours after docetaxel administration, we dissected the tumors and determined the amount of docetaxel incorporated into the tumors by HPLC with ultraviolet detection at 225 nm after solid-liquid extraction. We detected docetaxel in tumors that had received RPN2 siRNA ($n = 4$) at a range of 667 to 1400 ng per wet gram of tissue (**Fig. 4i**). In contrast, the tumors that received control siRNA ($n = 4$) showed a very low amount of docetaxel (~10 ng per wet gram of tissue). Thus, the results clearly indicate that abrogation of RPN2 expression in drug-resistant tumors results in docetaxel accumulation in those tumors.

### RPN2 siRNA reduces N-linked glycosylation of MDR1

The mammalian *RPN2* gene encodes a type I integral membrane protein found only in the rough endoplasmic reticulum[25,26]. The RPN2 protein is part of an *N*-oligosaccharyl transferase complex that links high mannose oligosaccharides to asparagine residues found in the N-X-S/T consensus motif of nascent polypeptide chains[27]. The expression of the multidrug transporter P-glycoprotein, encoded by *MDR1*, is one of the causes of clinical drug resistance to taxanes. Real-time RT-PCR analysis showed that MCF7-ADR cells expressed abundant MDR1 mRNA, whereas parental cells did not (**Fig. 3c**). In addition, the MDR1 mRNA amount was not significantly decreased
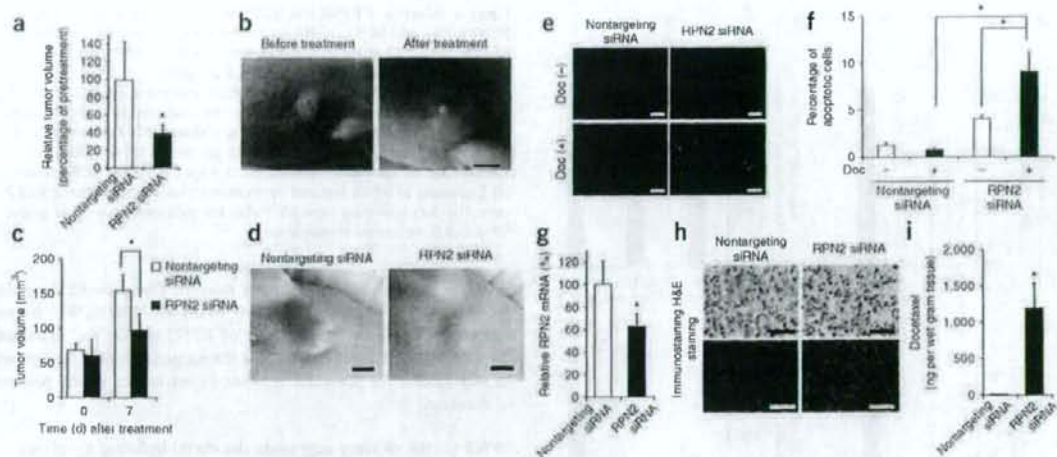
**Figure 4** Delivery of RPN2 siRNA to docetaxel-resistant breast tumors. The effect of RPN2 siRNA was examined in orthotopic breast tumor models. (a) Reduction of MCF7-ADR breast tumor volume in mice given RPN2 siRNA or control nontargeting siRNA along with docetaxel ($n = 6$ per group, *$P < 0.01$). (b) siRNA-treated MCF7-ADR tumors in mice before and 7 d after docetaxel treatment. Scale bar, 5 mm. (c) Growth of MDA-MB-231/MDR1 breast tumor in mice administered RPN2 siRNA or nontargeting siRNA along with docetaxel ($n = 6$ per group, *$P < 0.002$). (d) MDA-MB-231/MDR1 tumors in mice 7 d after treatment with siRNA and docetaxel. Scale bar, 5 mm. (e) TUNEL staining of MCF7-ADR tumor tissues treated with RPN2 siRNAs or nontargeting siRNAs in the presence or absence of docetaxel. Scale bar, 50 μm. (f) TUNEL-positive cells were counted and are represented in the graph ($n = 3$ per group, *$P < 0.01$). (g) Expression of RPN2 mRNA in MCF7-ADR tumors treated with RPN2 siRNAs or nontargeting siRNAs ($n = 3$ per group, *$P < 0.01$). (h) Expression of RPN2 protein in MCF7-ADR tumors. H&E staining and RPN2 immunofluorescence staining (green, RPN2; blue, nuclei) of tissues treated with RPN2 siRNA or nontargeting siRNA. Scale bar, 50 μm. (i) Docetaxel retention in MCF7-ADR tumors in mice treated with RPN2 siRNAs or nontargeting siRNAs ($n = 4$ per group, *$P < 0.001$). Values are means ± s.d.

in MCF7-ADR cells transduced by RPN2 siRNA (**Supplementary Fig. 4** online). For this reason, and to assess the potential involvement of *RPN2* gene overexpression in MDR1 functions, we tested the glycosylation status of MDR1 protein in MCF7-ADR cells transfected with RPN2 siRNA. We analyzed the glycosylation patterns by western blotting of P-glycoprotein, which appears on blots as mature 170-kDa, immature (partially glycosylated) 150-kDa and unglycosylated 140-kDa bands[28]. The 150-kDa immature and 140-kDa unglycosylated P-glycoproteins were clearly found in MCF7-ADR cells with RPN2 knockdown (90% inhibition of mRNA by real-time RT-PCR analysis; **Fig. 5a**). More than 80% of P-glycoproteins were unglycosylated or partially glycosylated in RPN2-silenced cells (composition of P-glycoproteins, 170 kDa:150 kDa:140 kDa = 18:40:42). In contrast, MCF7-ADR cells transduced with nontargeting control siRNA expressed more than half of their P-glycoproteins as170-kDa mature P-glycoprotein (170 kDa:150 kDa:140 kDa = 52:17:31). This result showed that RPN2 knockdown inhibits glycosylation of P-glycoproteins in MCF7-ADR cells. The western blot of P-glycoprotein, particularly in cells transduced with RPN2 siRNA, showed 'smear' patterns (**Fig. 5a**). We speculated that the smear pattern was caused by the presence of intermediately glycosylated forms in various sizes. We treated the cell lysate samples with peptide:N-glycosidase F (PNGase F) to remove N-glycan chains, which shifted the P-glycoprotein in the blot from a smear pattern to a 140-kDa unglycosylated protein band in MCF7-ADR cell lysates. After PNGase F treatment, both nontargeting control siRNA– and RPN2 siRNA–transduced cells showed a 140-kDa unglycosylated P-glycoprotein band (**Fig. 5a**). This indicates that the smear pattern resulted from the presence of intermediately glycosylated P-glycoprotein and that there were a number of

intermediately glycosylated P-glycoproteins in the RPN2-silenced cells because of inhibition of glycosylation on P-glycoprotein.

We further evaluated the RPN2 siRNA effects on cell surface P-glycoprotein expression in MCF7-ADR cells by immunofluorescence staining. As expected, immunofluorescence staining indicated that P-glycoprotein was predominantly localized to the cell membrane in MCF7-ADR cells transduced with control nontargeting siRNAs, whereas the intensity of membrane P-glycoprotein in RPN2-downregulated cells was considerably reduced (**Fig. 5b**). Moreover, retention of rhodamine-123, which is a substrate of P-glycoprotein, was strongly enhanced in MCF7-ADR cells transfected with RPN2 siRNA compared to those transfected with nontargeting siRNA (**Fig. 5c**). This indicates that downregulation of RPN2 restores drug retention and inhibits P-glycoprotein function by suppressing the glycosylation of P-glycoproteins in MCF7-ADR cells.

To further bolster these findings, we performed immunostaining analysis of RPN2 and P-glycoprotein in MCF7-ADR tumors in mice. The RPN2 shutdown resulted in a marked disappearance of the membrane-bound P-glycoprotein (**Fig. 5d**), an observation that supports our *in vitro* findings that RPN2 downregulation by siRNA in drug-resistant MCF7-ADR cells results in the loss of membrane-bound P-glycoprotein.

Furthermore, we have examined the status of RPN2 and P-glycoprotein in breast cancer tissues from subjects with RPN2 mRNA high expression ($n = 4$) and RPN2 mRNA low expression ($n = 4$) by immunostaining. P-glycoprotein was predominantly localized to the cell membrane in the primary tumor with a strong signal for RPN2, whereas in the primary tumor with low expression of RPN2, P-glycoprotein was found in the cytoplasm (**Supplementary**
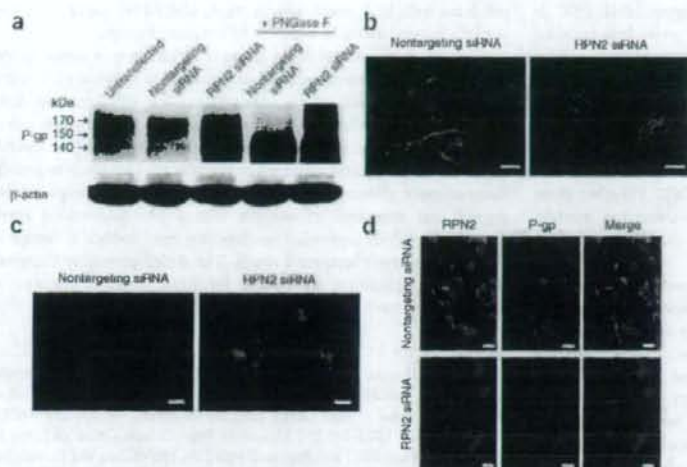
**Figure 5** RPN2 siRNA regulates glycosylation of P-glycoprotein (P-gp). (a) Western blot analysis shows the glycosylation status of P-gp in MCF7-ADR cells 72 h after transfection of RPN2 siRNA or control nontargeting siRNA. Bands migrating at 170, 150 and 140 kDa represent mature, immature and unglycosylated forms of P-gp, respectively. (b) Immunofluorescence staining of P-gp on MCF7-ADR cell membrane surfaces. Cells were treated with RPN2 siRNA or nontargeting siRNA for 72 h. Scale bar, 5 μm. (c) Rhodamine-123 retention in MCF7-ADR cells 72 h after transfection with RPN2 siRNA or control nontargeting siRNA. Scale bar, 5 μm. (d) Localization of P-gp in tumors of MCF7-ADR in mice. Immunofluorescence staining of RPN2 (green) and P-gp (red) are shown. Nuclei are blue (DAPI). Merged images are also shown. Scale bar, 5 μm.

Fig. 5a,b online). Similar results were observed for other breast cancer tissues (**Supplementary Fig. 5c**).

Thus, these data provide a clear link between the glycosylation status of P-glycoprotein and RPN2 expression in drug-resistant breast cancer cells, and the disappearance of the membrane-bound P-glycoprotein leads to a reversal of the multidrug- resistant phenotype.

## DISCUSSION

Cancer researchers today are confronted with how to best identify and select the next generation of molecular targets for oncology. An impressive array of potential new cellular targets, suitable for therapeutic intervention, has been revealed by the recent completion of the human genome sequencing project. Approaches as varied as transcription profiling, proteomics and the use of siRNAs are all being exploited in the race to select the most promising candidate drug targets. We tested the feasibility of using atelocollagen-mediated RNAi delivery in vitro and in vivo to obtain an unbiased evaluation on the efficacy of a specific siRNA related to drug resistance in human breast cancer. We show here that, among genes whose expression was elevated in nonresponders to docetaxel, the siRNA designed for RPN2 significantly promoted docetaxel-dependent apoptosis and cell growth inhibition of MCF7-ADR human breast cancer cells that exhibit docetaxel resistance. A clinicopathological study showed that there is a significant association of RPN2 expression with a pathologic response to docetaxel. Most notably, atelocollagen-mediated in vivo delivery of RPN2 siRNA significantly reduced the size of orthotopic MCF7-ADR tumors in mice given docetaxel.

In this study, we demonstrated that the atelocollagen delivery system markedly enhanced the efficiency of siRNA for the inhibition of RPN2 in mouse tumor models of human breast cancer. Because the

siRNA shows very low efficiency in gene silencing in vivo, various delivery methods, such as the use of plasmids and viral vectors encoding siRNA and the use of lipids, have been investigated. We have previously shown that the atelocollagen-mediated systemic delivery of siRNA might be a unique strategy for the inhibition of bone-metastatic prostate tumor growth[22]. The siRNA-atelocollagen complex is a nano-sized particle and is stable in vitro and in vivo[21,29]. Furthermore, we have previously confirmed that the atelocollagen complex shows low toxicity and low immunogenicity in vivo[23,24]. Thus, an atelocollagen-mediated local or systemic delivery system holds great potential for the practical application of gene suppression using siRNAs for cancer therapeutics.

Targeting of P-glycoprotein by small-molecular compounds, antibodies or both is an effective strategy to overcome multiple drug resistance in cancer[30]. Despite promising previous studies showing that the inhibition of P-glycoprotein by pharmacological means can sensitize drug-resistant cells, the ultimate goal of restoring drug sensitivity has met with limited success in clinical trials. Our results indicate that RPN2 is partly responsible for P-glycoprotein–mediated drug resistance in breast cancer and is involved in the regulation of the glycosylation status of P-glycoprotein. In fact, downregulation of RPN2 restored drug retention, suggesting that P-glycoprotein function is inhibited via suppression of the glycosylation of P-glycoprotein in MCF7-ADR cells. N-glycosylation has been shown to contribute to the stability of the P-glycoproteins[31], and it has been reported that reduced glycosylation results in the disappearance of membrane-bound P-glycoprotein, which causes the loss of a multidrug-resistant phenotype[32]. Furthermore, multidrug-resistant cells are hypersensitive to the N-linked glycosylation inhibitor tunicamycin, which induces partial inhibition of the glycosylation of GLUT-1, a glucose transporter, and diminishes GLUT-1–mediated transport[33]. Because the amount of MDR1 mRNA was not significantly decreased in MCF7-ADR cells transduced with RPN2 siRNA, it is predicted that RPN2 inhibition may reduce the glycosylation of P-glycoprotein, thereby inducing perturbation of its subcellular localization, inhibition of its protein synthesis and/or acceleration of its degradation, with MCF7-ADR cells inevitably becoming hypersensitive response to docetaxel. In contrast, the RPN2 protein is part of an N-oligosaccharyl transferase complex that links to N-glycosylation ability; therefore, RPN2 inhibition could affect N-oligosaccharyl transferase function, resulting in impaired glycosylation of the P-glycoproteins. We speculate that RPN2 has a key role in drug-resistant tumor cells that overexpress P-glycoprotein and acts as a facilitator, stabilizing factor or both for N-glycosylation of P-glycoprotein. The coordinated expression of RPN2 and P-glycoprotein may participate in the mechanism of docetaxel resistance via the glycosylation status of P-glycoprotein.

However, one group has recently reported that the stability of P-glycoprotein is regulated by the ubiquitin-proteasome pathway in multidrug-resistant cancer cells[34]. Furthermore, the P-glycoprotein must be phosphorylated by protein kinase C (PKC) to effectively

function as a drug-efflux pump[35], which suggests that PKC is indirectly involved in the development of the multidrug-resistant phenotype. More recently, it was revealed that wild-type p53, a tumor suppressor, may resensitize soft tissue sarcoma to chemotherapeutic agents by reducing MDR1 phosphorylation via transcriptional repression of PKC expression[36]. There is no direct evidence of RPN2 involvement with the transcriptional repression of PKC. Other transporter proteins mediating drug resistance are the multidrug resistance–associated protein and ABCG2. Whether these different populations of multidrug resistance–associated protein family members and ABCG2 are affected by RPN2 has yet to be determined.

Recently, downregulation of multidrug resistance by the introduction of synthetic siRNAs has been reported[37,38]. However, only partial reversal of the drug-sensitive phenotype of the cells has been obtained. A possible explanation for this low inhibitory effect is that it was the result of a long half-life of P-glycoprotein[39] and the less efficient delivery of synthetic siRNAs into cells. Although the data are not shown, we compared the cell growth inhibition by synthetic RPN2 siRNA versus MDR1 siRNA in the presence of docetaxel in vitro. At the mRNA level, the downregulation of RPN2 and MDR1 obtained with the most efficient siRNA was 90% and 80%, respectively. These results indicate that cell growth inhibition was achieved by both siRNAs, although RPN2 siRNA showed a stronger growth inhibitory effect compared to MDR1 siRNA. Thus, though it is impossible at the moment to judge whether MDR1 or RPN2 is a more profitable target for overcoming drug resistance, RPN2 does provide a valuable clue for making multidrug-resistant breast cancer cells sensitive to anticancer drugs.

The continuing interest in apoptosis among cancer biologists has been strengthened by the hope that a molecular understanding of cell death will inform our understanding of cancer drug resistance. In fact, upregulation of antiapoptotic Bcl2 family genes has been shown to be key in tumor malignancy and drug resistance[40,41]. Overexpression of exogenous Bcl-xL or Bcl-2 suppresses apoptosis[42,43]. In our study, knockdown of RPN2 by siRNA in MCF7-ADR cells selectively downregulated mRNA expression of Bcl-xL and Bcl-w (Supplementary Fig. 6 online). These results suggest that RPN2 regulates Bcl-xL– and Bcl-w–mediated antiapoptosis and may be partly responsible for the docetaxel resistance of the MCF7-ADR cells. It has already been reported that apoptosis-based therapies[44], such as the downregulation of Bcl-xL expression, Bcl-w expression or both with antisense oligonucleotides, abolish tumorigenicity and enhance chemosensitivity in human malignant glioma cells[45–47]. In addition, Bcl-xL and Bcl-w are upregulated by nuclear factor-κB (NF-κB)[48]. Some chemotherapeutic agents, such as cisplatin and docetaxel, instantly induce the activation of NF-κB in cancer cells, and the cells become drug resistant[49]. In fact, we found that RPN2 gene expression is also induced by docetaxel treatment of drug-sensitive MCF7 cells. Therefore, it would be useful to know whether RPN2 induces the downregulation of Bcl-xL and Bcl-w in MCF7-ADR cells by direct association with the NF-κB signaling pathway.

It is noteworthy that our findings using docetaxel-resistant human breast cancer cells are commonly found in other multiple cancers. Cisplatin-resistant human non–small cell lung carcinoma cells recover their sensitivity to cisplatin by knockdown of RPN2 expression and die by apoptosis (Y.Y., K.H. and T.O., unpublished data). In addition, mouse mammary tumor cells resistant to docetaxel express mouse Rpn2, and inhibition of Rpn2 results in apoptotic cell death in the presence of docetaxel (Supplementary Fig. 2e–g). Therefore, RPN2 status is responsible for the drug-resistant nature of multiple cancer

cell lines both in humans and in mice, and RPN2 expression may confer cross-resistance to a variety of anticancer drugs.

We previously reported that a group of redox genes is useful for the prediction of the clinical response to docetaxel in subjects with breast cancer[16]. Our current results indicate that the RPN2 mRNA level might serve as a predictor of the response to anticancer therapy rather than as a prognostic factor. The determination of the RPN2 mRNA level will be useful in the selection of subjects who are likely to benefit from adjuvant chemotherapy. Furthermore, our animal experiments suggest that treatment of subjects with a pharmacological agent that blocks RPN2 expression or function may induce a complete response to chemotherapeutic drugs. The RPN2 gene may therefore represent a promising new target for RNAi therapeutics against multidrug-resistant tumors.

## METHODS

**Cell culture.** Human mammary carcinoma cell lines, MCF7 cells and multidrug-resistant MCF7-ADR cells were provided by Shien-Lab, Medical Oncology, National Cancer Center Hospital of Japan. We cultured MCF7, MCF7-ADR and MDA-MB-231 (American Type Culture Collection) cells in RPMI 1640 (Gibco BRL) supplemented with 10% FBS (Gibco BRL) under 5% $CO_2$ in a humidified incubator at 37 °C. We cultured the mouse mammary tumor cell line EMT6/AR10.0 (European Collection of Cell Cultures), which shows docetaxel resistance, in MEM (EBSS) with 2 mM glutamine, 1% non essential amino acids and 10% FBS. The establishment of bioluminescent MCF7-ADR-Luc cells and docetaxel-resistant MDA-MB-231/MDR1 cells is described in Supplementary Methods online.

**Design and synthesis of small interfering RNAs.** We designed siRNAs and synthesized them with an siRNA duplex for each gene target (Dharmacon) for the preparation of an atelocollagen-based cell transfection array. The siRNA sequences are described in Supplementary Methods.

**Atelocollagen-based cell transfection array.** For RNAi-based functional screening, we prepared an atelocollagen-based cell transfection array, which enables reverse transfection of cells by atelocollagen-mediated gene transfer (Supplementary Methods). We performed live-cell luciferase assay for measurement of cell growth, and we performed caspase-7 assays with Apo-ONE Caspase-3/7 Assay Reagent (Promega) and Hoechst staining for apoptosis (Supplementary Methods).

**Real-time reverse transcription PCR.** We purified total RNA from cells and tumor tissues with an RNeasy Mini Kit and RNase-Free DNase Set (QIAGEN) and produced cDNAs with an ExScript RT reagent Kit (Takara). We then subjected cDNA samples to real-time PCR with SYBR Premix Ex Taq (Takara) and specific primers (Supplementary Methods). We carried out the reactions in a LightCycler (Roche Diagnostics). We normalized gene expression levels by HPRT1 or ACTB. The cell-direct quantitative RT-PCR method is described in the Supplementary Methods.

**Atelocollagen-mediated RPN2 small interfering RNA delivery in vivo.** We performed mouse experiments in compliance with the guidelines of the Institute for Laboratory Animal Research at the National Cancer Center Research Institute of Japan. We used 4-week-old female athymic nude mice (CLEA Japan) to generate an experimental orthotopic breast cancer model. We injected $1.0 \times 10^7$ MCF7-ADR cells or MDA-MB-231/MDR1 cells suspended in 100 μl sterile PBS into the fat pad. When the tumor grew to approximately 5 mm in diameter, we injected mice with 200 μl of siRNA-atelocollagen by intratumoral injection. Preparation of the siRNA-atelocollagen complex is described in the Supplementary Methods. Simultaneously, we injected docetaxel i.p. into mice. We harvested tumor tissues for analysis of RPN2 mRNA and RPN2 protein at 24 h and 72 h after treatment, respectively.

**TUNEL technique.** We harvested tumor tissues 72 h after administration of siRNA and prepared frozen sections. We then performed TUNEL staining with an in situ Cell Death Detection Kit, Fluorescein (Roche Diagnostics), according to the manufacturer's protocol. We stained the nuclei with DAPI. We

determined the number of fluorescein-positive cells in three microscopic fields of each section by fluorescence microscopy.

**Docetaxel disposition in tumors.** We studied drug disposition of docetaxel in tumors in mice by HPLC with ultraviolet detection at 225 nm after solid-liquid extraction as described elsewhere[50]. Eleven hours after i.p. administration of 20 mg kg^{-1} docetaxel, we harvested the tumors treated with siRNA-atelocollagen complex and then analyzed the docetaxel abundance in the tumor.

**Transfection of small interfering RNA.** We carried out transfection of MCF7-ADR and EMT6/AR10.0 cells with siRNA using DharmaFECT 1 (Dharmacon) and TransIT-TKO (Mirus), respectively, according to the manufacturers' protocol (Supplementary Methods).

**Antibodies.** We used RPN2-specific antibody (H300, Santa Cruz Biotechnology) and MDR-specific antibody (G-1, Santa Cruz Biotechnology). We visualized staining with Alexa 488 or Alexa 594 (Molecular Probes). We used fluorescence microscopy or confocal fluorescence microscopy (Olympus) for observation of immunofluorescence-stained cells. The procedures of western blotting and immunofluorescence staining are described in the Supplementary Methods.

**Rhodamine-123 retention assay.** We washed cells once with prewarmed Opti-MEM I medium (37 °C, Gibco BRL) and incubated the cells for 30 min at 37 °C in the Opti-MEM I medium containing 10 μM rhodamine-123. We then removed the rhodamine-123 solution from the extracellular medium and washed the cells twice with Opti-MEM I medium. We observed the cells for fluorescence of rhodamine-123 under fluorescence microscopy.

**Human samples.** The study protocol for clinical samples (results presented in Table 1) was approved by the Institutional Review Board of Osaka University Medical School, and written informed consent was obtained from each subject (Supplementary Note).

**Statistical analyses.** We conducted statistical analysis by analysis of variance with the Student's t-test. We considered a P value of 0.05 or less as a significant difference.

*Note: Supplementary information is available on the Nature Medicine website.*

### AUTHOR CONTRIBUTIONS
K.H. performed the experimental work, data analysis and writing of the first draft of the manuscript. K.K. and T.O. selected the initial set of genes subjected to the screening. K.I.-K., K.K., T.Y. and T.O. participated in the conception, design and coordination of the study. P.T. and Y.Y. performed siRNA delivery *in vivo* and helped with data analysis. K.N. provided drug-resistant cell lines. S.N. provided delivery molecules. The manuscript was finalized by T.O. with the assistance of all authors.

1. Kaufmann, M. *et al.* International expert panel on the use of primary (preoperative) systemic treatment of operable breast cancer: review and recommendations. *J. Clin. Oncol.* 21, 2600–2608 (2003).
2. Gradishar, W.J. *et al.* Neoadjuvant docetaxel followed by adjuvant doxorubicin and cyclophosphamide in patients with stage III breast cancer. *Ann. Oncol.* 16, 1297–1304 (2005).
3. Formenti, S.C. *et al.* Preoperative twice-weekly paclitaxel with concurrent radiation therapy followed by surgery and postoperative doxorubicin-based chemotherapy in locally advanced breast cancer: A phase I/II trial. *J. Clin. Oncol.* 21, 864–870 (2003).
4. Engels, F.K., Sparreboom, A., Mathot, R.A. & Verweij, J. Potential for improvement of docetaxel-based chemotherapy: a pharmacological review. *Br. J. Cancer* 93, 173–177 (2005).
5. Crown, J., O'Leary, M. & Ooi, W.S. Docetaxel & paclitaxel in the treatment of breast cancer: a review of clinical experience. *Oncologist* 9, 24–32 (2004).
6. Jones, S.E. *et al.* Randomized phase III study of docetaxel compared with paclitaxel in metastatic breast cancer. *J. Clin. Oncol.* 23, 5542–5551 (2005).
7. Bonneterre, J. *et al.* Efficacy and safety of docetaxel (Taxotere) in heavily pretreated advanced breast cancer patients: the French compassionate use programme experience. *Eur. J. Cancer* 35, 1431–1439 (1999).
8. Gottesman, M.M., Pastan, I. & Ambudkar, S.V. P-glycoprotein and multidrug resistance. *Curr. Opin. Genet. Dev.* 6, 610–617 (1996).
9. Duan, Z., Brakora, K.A. & Seiden, M.V. Inhibition of ABCB1 (MDR1) and ABCB4 (MDR3) expression by small interfering RNA and reversal of paclitaxel resistance in human ovarian cancer cells. *Mol. Cancer Ther.* 3, 833–838 (2004).
10. Leslie, E.M., Deeley, R.G. & Cole, S.P. Toxicological relevance of the multidrug resistance protein 1, MRP1 (ABCC1) and related transporters. *Toxicology* 167, 3–23 (2001).
11. Renes, J., de Vries, E.G., Jansen, P.L. & Muller, M. The (patho)physiological functions of the MRP family. *Drug Resist. Updat.* 3, 289–302 (2000).
12. Leonessa, F. & Clarke, R. ATP binding cassette transporters and drug resistance in breast cancer. *Endocr. Relat. Cancer* 10, 43–73 (2003).
13. Lin, J.C., Chang, S.Y., Hsieh, D.S., Lee, C.F. & Yu, D.S. The association of Id-1, MIF and GSTpi with acquired drug resistance in hormone independent prostate cancer cells. *Oncol. Rep.* 13, 983–988 (2005).
14. Galimberti, S., Testi, R., Guerrini, F., Fazzi, R. & Petrini, M. The clinical relevance of the expression of several multidrug-resistant-related genes in patients with primary acute myeloid leukemia. *J. Chemother.* 15, 374–379 (2003).
15. Burg, D., Riepsaame, J., Pont, C., Mulder, G. & van de Water, B. Peptide-bond modified glutathione conjugate analogs modulate GSTpi function in GSH-conjugation, drug sensitivity and JNK signaling. *Biochem. Pharmacol.* 71, 268–277 (2006).
16. Iwao-Koizumi, K. *et al.* Prediction of docetaxel response in human breast cancer by gene expression profiling. *J. Clin. Oncol.* 23, 422–431 (2005).
17. Kim, S.J. *et al.* High thioredoxin expression is associated with resistance to docetaxel in primary breast cancer. *Clin. Cancer Res.* 11, 8425–8430 (2005).
18. Kato, K. Adaptor-tagged competitive PCR: a novel method for measuring relative gene expression. *Nucleic Acids Res.* 25, 4694–4696 (1997).
19. Honma, K. *et al.* Atelocollagen-based gene transfer in cells allows high-throughput screening of gene functions. *Biochem. Biophys. Res. Commun.* 289, 1075–1081 (2001).
20. Honma, K., Miyata, T. & Ochiya, T. The role of atelocollagen-based cell transfection array in high-throughput screening of gene functions and in drug discovery. *Curr. Drug Discov. Technol.* 1, 287–294 (2004).
21. Minakuchi, Y. *et al.* Atelocollagen-mediated synthetic small interfering RNA delivery for effective gene silencing *in vitro* and *in vivo*. *Nucleic Acids Res.* 32, e109 (2004).
22. Takeshita, F. *et al.* Efficient delivery of small interfering RNA to bone-metastatic tumors by using atelocollagen *in vivo*. *Proc. Natl. Acad. Sci. USA* 102, 12177–12182 (2005).
23. Ochiya, T. *et al.* New delivery system for plasmid DNA *in vivo* using atelocollagen as a carrier material: the Minipellet. *Nat. Med.* 5, 707–710 (1999).
24. Ochiya, T., Nagahara, S., Sano, A., Itoh, H. & Terada, M. Biomaterials for gene delivery: atelocollagen-mediated controlled release of molecular medicines. *Curr. Gene Ther.* 1, 31–52 (2001).
25. Crimaudo, C., Hortsch, M., Gausepohl, H. & Meyer, D.I. Human ribophorins I and II: the primary structure and membrane topology of two highly conserved rough endoplasmic reticulum-specific glycoproteins. *EMBO J.* 6, 75–82 (1987).
26. Kelleher, D.J., Kreibich, G. & Gilmore, R. Oligosaccharyltransferase activity is associated with a protein complex composed of ribophorins I and II and a 48 kd protein. *Cell* 69, 55–65 (1992).
27. Kelleher, D.J. & Gilmore, R. An evolving view of the eukaryotic oligosaccharyltransferase. *Glycobiology* 16, 47R–62R (2006).
28. Loo, T.W., Bartlett, M.C. & Clarke, D.M. The dileucine motif at the COOH terminus of human multidrug resistance P-glycoprotein is important for folding but not activity. *J. Biol. Chem.* 280, 2522–2528 (2005).
29. Ochiya, T., Honma, K., Takeshita, F. & Nagahara, S. Atelocollagen-mediated drug discovery technology. *Expert Opin. Drug Discov.* 2, 159–167 (2007).
30. Tsuruo, T. *et al.* Molecular targeting therapy of cancer: drug resistance, apoptosis and survival signal. *Cancer Sci.* 94, 15–21 (2003).
31. Schinkel, A.H., Kemp, S., Dolle, M., Rudenko, G. & Wagenaar, E. N-glycosylation and deletion mutants of the human MDR1 P-glycoprotein. *J. Biol. Chem.* 268, 7474–7481 (1993).
32. Kramer, R. *et al.* Inhibition of N-linked glycosylation of P-glycoprotein by tunicamycin results in a reduced multidrug resistance phenotype. *Br. J. Cancer* 71, 670–675 (1995).
33. Bentley, J., Quinn, D.M., Pitman, R.S., Warr, J.R. & Kellett, G.L. The human KB multidrug-resistant cell line KB-C1 is hypersensitive to inhibitors of glycosylation. *Cancer Lett.* 115, 221–227 (1997).
34. Zhang, Z., Wu, J.Y., Hait, W.N. & Yang, J.M. Regulation of the stability of P-glycoprotein by ubiquitination. *Mol. Pharmacol.* 66, 395–403 (2004).

# ARTICLES

35. O'Brian, C.A., Ward, N.E., Stewart, J.R. & Chu, F. Prospects for targeting protein kinase C isozymes in the therapy of drug-resistant cancer—an evolving story. *Cancer Metastasis Rev.* **20**, 95–100 (2001).
36. Zhan, M. *et al.* Transcriptional repression of protein kinase Cα via Sp1 by wild type p53 is involved in inhibition of multidrug resistance 1 P-glycoprotein phosphorylation. *J. Biol. Chem.* **280**, 4825–4833 (2005).
37. Nieth, C., Priebsch, A., Stege, A. & Lage, H. Modulation of the classical multidrug resistance (MDR) phenotype by RNA interference (RNAi). *FEBS Lett.* **545**, 144–150 (2003).
38. Wu, H., Hait, W.N. & Yang, J.M. Small interfering RNA–induced suppression of MDR1 (P-glycoprotein) restores sensitivity to multidrug-resistant cancer cells. *Cancer Res.* **63**, 1515–1519 (2003).
39. Muller, C., Laurent, G. & Ling, V. P-glycoprotein stability is affected by serum deprivation and high cell density in multidrug-resistant cells. *J. Cell. Physiol.* **163**, 538–544 (1995).
40. Pommier, Y., Sordet, O., Antony, S., Hayward, R.L. & Kohn, K.W. Apoptosis defects and chemotherapy resistance: molecular interaction maps and networks. *Oncogene* **23**, 2934–2949 (2004).
41. Sordet, O., Khan, Q.A., Kohn, K.W. & Pommier, Y. Apoptosis induced by topoisomerase inhibitors. *Curr. Med. Chem. Anticancer Agents* **3**, 271–290 (2003).
42. Schott, A.F., Apel, I.J., Nunez, G. & Clarke, M.F. Bcl-XL protects cancer cells from p53-mediated apoptosis. *Oncogene* **11**, 1389–1394 (1995).

43. Walczak, H., Bouchon, A., Stahl, H. & Krammer, P.H. Tumor necrosis factor-related apoptosis-inducing ligand retains its apoptosis-inducing capacity on Bcl-2– or Bcl-xL–overexpressing chemotherapy-resistant tumor cells. *Cancer Res.* **60**, 3051–3057 (2000).
44. Reed, J.C. Apoptosis-based therapies. *Nat. Rev. Drug Discov.* **1**, 111–121 (2002).
45. Lytle, R.A., Jiang, Z., Zheng, X. & Rich, K.M. BCNU down-regulates anti-apoptotic proteins Bcl-xL and Bcl-2 in association with cell death in oligodendroglioma-derived cells. *J. Neurooncol.* **68**, 233–241 (2004).
46. Jiang, Z., Zheng, X. & Rich, K.M. Down-regulation of Bcl-2 and Bcl-xL expression with bispecific antisense treatment in glioblastoma cell lines induce cell death. *J. Neurochem.* **84**, 273–281 (2003).
47. Guensberg, P. *et al.* Bcl-xL antisense oligonucleotides chemosensitize human glioblastoma cells. *Chemotherapy* **48**, 189–195 (2002).
48. Tran, N.L. *et al.* The tumor necrosis factor-like weak inducer of apoptosis (TWEAK)-fibroblast growth factor-inducible 14 (Fn14) signaling system regulates glioma cell survival via NFκB pathway activation and BCL-XL/BCL-W expression. *J. Biol. Chem.* **280**, 3483–3492 (2005).
49. Li, Y. *et al.* Inactivation of nuclear factor κB by soy isoflavone genistein contributes to increased apoptosis induced by chemotherapeutic agents in human cancer cells. *Cancer Res.* **65**, 6934–6942 (2005).
50. Vergniol, J.C., Bruno, R., Montay, G. & Frydman, A. Determination of Taxotere in human plasma by a semi-automated high-performance liquid chromatographic method. *J. Chromatogr.* **582**, 273–278 (1992).

# S-1 Treatment for Chemorefractory Thymic Carcinoma

**To the Editor:**

Thymic carcinoma is a rare and invasive mediastinal neoplasm that often metastasizes. Recently, Yano et al.[1] reported in this journal that unresectable thymic carcinoma has an extremely poor prognosis. In addition, the treatment options for unresectable thymic carcinoma are extremely limited because of the lack of evidence about effective treatments even in the first-line setting. We describe a case of unresectable thymic carcinoma that showed good response to S-1 treatment after failure of prior chemotherapies.

A 67-year-old man with unresectable thymic carcinoma was admitted to our hospital for fourth-line treatment. The patient had been well until 3 years earlier, when he developed persistent chest discomfort. A chest computed tomography (CT) at that time revealed an anterior mediastinal mass along with multiple pulmonary nodules; a computed tomography guided biopsy of the anterior mediastinal mass revealed a tumor composed of large-sized atypical epithelial cells arranged in nests and separated by abundant connective tissue. Immunohistochemical analysis showed tumor cell positivity for CD5 and AE1/3. The findings were consistent with a diagnosis of thymic squamous cell carcinoma, stage IVb (Masaoka's staging system). The patient was treated with multiple chemotherapy regimens, including carboplatin with paclitaxel, amrubicin, and gemcitabine; the best objective tumor response was stable disease as assessed by the Response Evaluation Criteria in Solid Tumors. The tumor regrew after the treatments, necessitating additional palliative treatment. Therefore, S-1 was administered orally after meals at a dose of 40 mg/m$^2$ twice

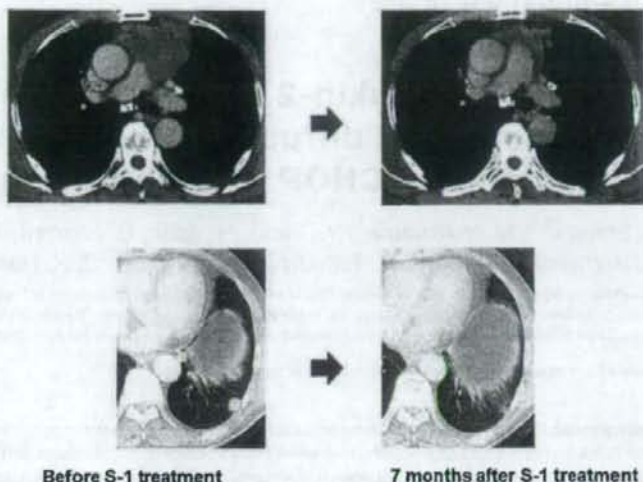**Before S-1 treatment**       **7 months after S-1 treatment**

**FIGURE 1.** CT findings obtained before and 7 months after S-1 treatment.

daily. Each course consisted of consecutive administration of S-1 for 28 days, followed by a 14-day drug-free interval. The treatment was continued until disease progression or appearance of prohibitive toxicity. Grade two thrombocytopenia and grade two nausea were noted (National Cancer Institute-common toxicity criteria version 3.0). In regard to the tumor response, the mediastinal tumor markedly shrank in size and the pulmonary metastases disappeared; partial response was obtained after the second course (Figure 1). At present, 8 months after the start of treatment, the patient remains well with maintained partial response status.

Although some chemotherapeutic agents including pemetrexed or gefitinib have been recently reported to be effective against pretreated thymic carcinoma, the response rate to these treatments remains low (18 and 4%, respectively).[2,3] S-1 (TS-1; Taiho Pharmaceutical, Tokyo, Japan) is a new oral anticancer agent that contains a mixture of the 5-FU prodrug tegafur and two enzyme inhibitors, 5-chloro-2,4-dihydroxypyridine and potassium oxonate, at the molar ratio of 1:0.4:1.5. S-1 has been reported to be effective in the treatment of various solid tumors, including gastric cancer, colon cancer, and non-small-cell lung cancer.[4,5] The anticancer activity of 5-FU has been reported to be closely related to

the intratumoral expression of thymidylate synthase and dihydropyrimidine dehydrogenase.[5] Although the precise expression profiles of these enzymes in thymic cell carcinoma have not been determined yet, S-1 might show favorable anticancer activities, as in this case. Further clinical studies are needed to confirm our result.

**Akira Ono, MD**
**Tateaki Naito, MD, PhD**
**Nobuyuki Yamamoto, MD, PhD**
Division of Thoracic Oncology
Shizuoka Cancer Center
Shizuoka
Japan

## REFERENCES

1. Yano M, Sasaki H, Yokoyama T, et al. Thymic carcinoma: 30 cases at a single institution. *J Thorac Oncol* 2008;3:265–269.
2. Kurup A, Burns M, Dropcho S, et al. Phase II study of Gefitinib treatment in advanced thymic malignancies. *Am Soc Clin Oncol* 2005; 23:7068 (abstract).
3. Loehrer PJ, Yiannoutsos CT, Dropcho S, et al. A phase II trial of pemetrexed in patients with recurrent thymoma or thymic carcinoma. *Am Soc Clin Oncol* 2006;24:7079 (abstract).
4. Kawahara M, Furuse K, Segawa Y, et al. Phase II study of S-1, a novel oral fluorouracil, in advanced non-small-cell lung cancer. *Br J Cancer* 2001;85:939–943.
5. Miyamoto S, Boku N, Ohtsu A, et al. Clinical implications of immunoreactivity of thymidylate synthase and dihydropyrimidine dehydrogenase in gastric cancer treated with oral fluoropyrimidine (S-1). Study Group of S-1 for Gastric Cancer. *Int J Oncol* 2000;17:653–658.

489

# original article

## Soluble interleukin-2 receptor retains prognostic value in patients with diffuse large B-cell lymphoma receiving rituximab plus CHOP (RCHOP) therapy

D. Ennishi[1,5], M. Yokoyama[1], Y. Terui[1], H. Asai[1], S. Sakajiri[1], Y. Mishima[1], S. Takahashi[1], H. Komatsu[2], K. Ikeda[3], K. Takeuchi[4], M. Tanimoto[5] & K. Hatake[1*]

[1]Department of Medical Oncology and Hematology, Cancer Institute Hospital, Tokyo; [2]Department of Epidemiology; [3]Department of Transfusion Medicine, Okayama University Graduate School of Medicine, Dentistry and Pharmaceutical Sciences, Okayama; [4]Devision of Pathology, The Japanese Foundation for Cancer Research, Tokyo; [5]Department of Hematology and Oncology, Okayama University Graduate School of Medicine, Dentistry and Pharmaceutical Sciences, Okayama, Japan

**Background:** Soluble interleukin-2 receptor (SIL-2R) is known to be a prognostic parameter in patients with diffuse large B-cell lymphoma (DLBCL) receiving cyclophosphamide, doxorubicin, vincristine and prednisone (CHOP) therapy. However, its prognostic value has not been well known since the introduction of rituximab.

**Patients and methods:** We retrospectively evaluated the prognostic impact of SIL-2R in 228 DLBCL patients, comparing 141 rituximab-combined CHOP (RCHOP)-treated patients with 87 CHOP-treated patients as a historical control.

**Results:** Patients with high serum SIL-2R showed significantly poorer event-free survival (EFS) and overall survival (OS) than patients with low SIL-2R in both the RCHOP group (2-year EFS, 66% versus 92%, $P < 0.001$; OS, 82% versus 95%, $P = 0.005$) and the CHOP group (2-year EFS, 40% versus 82%; OS, 61% versus 90%, both $P < 0.001$). Multivariate analysis including the five parameters of International Prognostic Index (IPI) and two-categorized IPI revealed that SIL-2R was an independent prognostic factor for EFS and OS in the RCHOP group as well as in the CHOP group.

**Conclusions:** Our results demonstrate that SIL-2R retains its prognostic value in the rituximab era. The prognostic value of SIL-2R in DLBCL patients receiving rituximab-combined chemotherapy should be reassessed on a larger scale and by long-term follow-up.

**Key words:** diffuse large B-cell lymphoma, rituximab, soluble interleukin-2 receptor

## introduction

Diffuse large B-cell lymphoma (DLBCL) is the most common subtype of non-Hodgkin's lymphoma [1]. It takes an aggressive clinical course and comprises a heterogeneous group of lymphomas in terms of morphology, phenotype, molecular biology and clinical behavior. Up to now, the International Prognostic Index (IPI) has been the most widely used predictive model for patients with DLBCL treated with cyclophosphamide, doxorubicin, vincristine and prednisone (CHOP) [2]. On the other hand, soluble interleukin-2 receptor (SIL-2R) has also been investigated as a prognostic factor, and several studies have demonstrated that a high level of SIL-2R before treatment is associated with both a low remission rate and poor prognosis [3–8].

SIL-2R is the soluble form of interleukin-2 receptor (IL-2R). IL-2R is expressed on the cell membrane of lymphocytes and plays important roles in their activation and proliferation [9]. It is composed of at least three glycoprotein chains: α (55 kDa), β (75 kDa) and γ (64 kDa). Each subunit is able to bind to the ligand independently with either low (IL-2Rα) or intermediate (IL-2Rβ and γ) affinity. It is now possible to examine the expression of the soluble-type α subunit [10]. The soluble IL-2Rα chain is induced and expressed only after mononuclear cell (T cell, B cell, monocyte, and natural killer cell) activation [11, 12]. Therefore, activated T and B cells have elevated levels of SIL-2R.

Although the CHOP regimen has been the mainstay of treatment for aggressive lymphomas for several decades [13], treatment outcome has significantly improved with the introduction of rituximab (an anti-CD20 chimeric antibody) in both young and elderly patients [14–17]. Since the introduction of rituximab, several prognostic factors have been reevaluated. Sehn et al. [18] recently reevaluated five prognostic

*Correspondence to: Dr Kiyohiko Hatake, Department of Medical Oncology and Hematology, Cancer Institute Hospital, 3-10-6 Ariake Koto-ku, Tokyo 135-8550, Japan. Tel: +81-3-3520-0111; Fax: +81-3-3570-0343; E-mail: khatake@jfcr.or.jp

factors and demonstrated that the IPI remained predictive; they proposed a revised IPI in which DLBCL patients are classified into very good (no IPI risk factors), good (one to two risk factors) and poor (three to five risk factors) categories. In contrast, BCL2, BCL6 and immunohistochemically defined germinal center (GC) phenotype have been reported to have no prognostic value when rituximab is added to chemotherapy [19–24]. Other clinical factors or biomarkers identified in patients receiving CHOP therefore need to be reassessed in patients treated with CHOP combined with rituximab.

Up to now, the prognostic value of SIL-2R in RCHOP has not been investigated. The aim of the present study was to retrospectively reassess the prognostic value of SIL-2R in DLBCL patients receiving RCHOP as compared with CHOP alone and to investigate whether or not this factor still influences the outcome of DLBCL.

## patients and methods

### patient characteristics

In the present study, we reviewed the medical records of patients with CD20-positive DLBCL who received CHOP with or without rituximab as a first-line therapy at the Cancer Institute Hospital from January 2000 to December 2006 and were followed until January 2008. The study protocol and sampling were approved by the Institutional Review Board of the Cancer Institute Hospital. Informed consent for retrospective analysis and additional immunophenotypic analysis and gene rearrangement studies was obtained.

Patients were analyzed if they were older than 18 years and had a performance status (PS) of zero to three according to the criteria of the European Cooperative Oncology Group. Patients were excluded if they had clinically relevant cardiac diseases or positivity for antibodies against HIV-1 or 2. Patients with primary mediastinal large B-cell lymphoma, primary CNS lymphoma and primary testicular lymphoma were also not included in this study.

The disease stage was evaluated according to the Ann Arbor staging system. All patients had undergone staging investigations, including physical examinations, blood and serum analysis, bone marrow aspiration and biopsy and computed tomography of the neck, chest, abdomen and pelvis. Magnetic resonance imaging was used for evaluation of involved organs in the head and neck. The following clinical and laboratory data were available at the time of diagnosis: age, sex, serum lactate dehydrogenase level, PS, presence of B symptoms, clinical stage and number of extranodal sites. This allowed the IPI scores to be determined in the studied patients. Patients were categorized into either a low-risk group (IPI score, 0–2) or a high-risk group (IPI score, 3–5). Response to initial therapy was evaluated according to the Cheson criteria [25].

### treatment

In both the CHOP and RCHOP groups, CHOP chemotherapy was given triweekly at a standard dose. Patients with stages IB–IV received six cycles, and patients with stage IA three cycles, of CHOP chemotherapy followed by radiotherapy for the involved field. After incorporation of rituximab into the CHOP regimen in February 2004, patients were treated with RCHOP regimen, in which rituximab was administered at a standard dose of 375 mg/m$^2$ once weekly for 8 weeks concurrently with triweekly CHOP, as described previously [26].

### chemical studies

The serum SIL-2R levels were determined using a sandwich enzyme-linked immunosorbent assay kit (Cell-free Interleukin-2 Receptor Test Kit, T Cell Science, Cambridge, MA) using two mAbs against distinct two different epitopes of the p55 alpha-chain of the IL-2R complex. Serum SIL-2R was considered 'high' when higher than the median and 'low' when lower than the median.

### pathological studies

Biopsy samples collected before treatment were fixed in formalin, embedded in paraffin, sliced and stained with hematoxylin and eosin for morphological analysis. For diagnosis of DLBCL, immunohistochemical analysis was carried out using the dextran-polymer method (EnVision+; Dako, Glostrup, Denmark) with mAbs against CD5, CD10, CD20, Ki67, BCL2, BCL6 and MUM1 in most cases and with CyclinD1 to exclude the possibility of a pleomorphic variant of mantle cell lymphoma when the lymphoma was CD5 positive. Patients with a small-cell component implying transformation from low-grade/indolent B-cell lymphoma were excluded. All the samples were reviewed by an expert hematopathologist (KT).

### statistical analysis

Basic characteristics of the CHOP group and RCHOP group were compared by Fisher's exact test. Event-free survival (EFS) was calculated from the date of diagnosis to the date of documented disease progression, relapse or death from any cause or to the stopping date. Overall survival (OS) was calculated from the date of diagnosis until death from any cause or the last follow-up. If the stopping date was not reached, the data were censored at the date of the last follow-up evaluation. Survival curves were estimated by the Kaplan–Meier method, and overall differences were compared by the log-rank test. Log-rank test was carried out according to SIL-2R, two-categorized IPI for the two treatment groups. To estimate the unbiased prognostic impacts of SIL-2R on EFS and OS, Cox proportional hazards analysis was applied. First, we conducted univariate Cox analysis for SIL-2L, all IPI factors and dichotomized IPI and then we carried out multivariate Cox analysis adjusted for SIL-2R and each of the IPI risk factors, with final adjustment for SIL-2R and dichotomized IPI. Only factors that were associated with at least a trend toward significance in the univariate analysis (unadjusted $P$ value <0.20) were evaluated in the multivariate model. We set $P$ <0.05 as the level of statistical significance. Data were analyzed using SPSS software version 11.0 for Windows (SPSS, Chicago, IL).

## results

### patient characteristics

A total of 228 patients were analyzed, of whom 87 (38.2%) were given CHOP and 141 (61.8%) were given RCHOP. The median SIL-2R was 1005.5 mg/dl (range 220–35 600), and high SIL-2R was observed in 114 (50.0%) patients: 40 of 87 (46.0%) in the CHOP group and 74 of 141 (52.5%) in the RCHOP group. There was no significant difference in the proportion of high SIL-2R patients between the two treatment groups. The characteristics of the patients are listed in Table 1. Patient and disease characteristics were well balanced between the groups.

### survival analysis

With median follow-up periods of 30 months in the RCHOP group and 44 months in the CHOP group, EFS rates at 2 years were 78% and 65%, respectively ($P = 0.030$), and OS rates at 2 years were 89% and 81%, respectively ($P = 0.040$).

# original article

**Table 1.** Patients' characteristics according to serum SIL-2R level for CHOP and RCHOP group

| Characteristics | CHOP group | | | RCHOP group | | | P, all |
|---|---|---|---|---|---|---|---|
| | All | Low SIL2R | High SIL2R | All | Low SIL2R | High SIL2R | |
| No. of patients (%) | 87(100) | 47 (54) | 40 (46) | 141 (100) | 67 (48) | 74 (52) | |
| Sex, no. (%) | | | | | | | 0.41 |
| Male | 50 (57) | 27 (57) | 23 (58) | 72 (51) | 27 (40) | 45 (61) | |
| Female | 37 (43) | 20 (43) | 17 (42) | 69 (49) | 40 (60) | 29 (39) | |
| Age, no. (%) | | | | | | | 0.52 |
| ≤60 | 24 (28) | 13 (28) | 11 (28) | 45 (32) | 29 (43) | 16 (22) | |
| >60 | 63 (72) | 34 (72) | 29 (72) | 96 (68) | 38 (57) | 58 (78) | |
| LDH, no. (%) | | | | | | | 0.54 |
| Normal | 29 (32) | 22 (35) | 7 (17) | 68 (48) | 45 (67) | 23 (31) | |
| High | 58 (68) | 25 (65) | 33 (83) | 73 (52) | 22 (33) | 51 (69) | |
| PS, no. (%) | | | | | | | 0.81 |
| 0–1 | 77 (89) | 44 (94) | 33 (83) | 127 (90) | 66 (98) | 61 (82) | |
| 2–3 | 10 (11) | 3 (6) | 7 (17) | 14 (10) | 1 (2) | 13 (18) | |
| Stage, no. (%) | | | | | | | 0.73 |
| I, II | 55 (63) | 40 (85) | 15 (38) | 93 (66) | 57 (85) | 36 (49) | |
| III, IV | 32 (37) | 7 (15) | 25 (72) | 48 (34) | 10 (15) | 38 (51) | |
| Extranodal sites, no. (%) | | | | | | | 0.84 |
| 0, 1 | 67 (77) | 43 (91) | 24 (60) | 106 (75) | 63 (94) | 43 (57) | |
| ≤2 | 20 (23) | 4 (9) | 16 (40) | 35 (25) | 4 (6) | 31 (43) | |
| IPI, no. (%) | | | | | | | 0.86 |
| L/L-I | 60 (69) | 40 (85) | 20 (50) | 100 (71) | 63 (94) | 37 (50) | |
| H/H-I | 27 (31) | 7 (15) | 20 (50) | 41 (29) | 4 (6) | 37 (50) | |

SIL2R, soluble interleukin-2 receptor; CHOP, cyclophosphamide, doxorubicin, vincristine and prednisone; RCHOP, rituximab-combined CHOP; LDH, lactate dehydrogenase; PS, performance status; IPI, International Prognostic Index; L/L-I, low or low-intermediate; H/H-I, high or high-intermediate; high SIL-2R; SIL-2R >1000 U/ml, low SIL-2R; SIL-2R ≤1000 U/ml.

For CHOP therapy, the EFS and OS rates at 2 years were 82% and 93% for low SIL-2R and 43% and 65% for high SIL-2R, respectively. The differences in both the EFS and OS rates between the two SIL-2R levels were significant (both $P < 0.001$) (Figure 1A and B). In the RCHOP group, the EFS and OS rates at 2 years were 90% and 95% for low SIL-2R and 66% and 84% for high SIL-2R, respectively. The differences in both EFS and OS rates between the two SIL-2R levels were significant (EFS, $P < 0.001$; OS $P = 0.005$) (Figure 1C and D).

To study the impact of rituximab on the predictive value, we examined the clinical outcome according to treatment in the SIL-2R low and high groups. The patients with high SIL-2R who received RCHOP therapy had a significantly better OS at 2 years than patients treated with CHOP alone (84% versus 65%, $P = 0.020$). The EFS at 2 years was estimated to be 66% for the RCHOP group and 43% for the CHOP group ($P = 0.010$). For the patients with low SIL-2R, the influence of rituximab on OS and EFS was not significant (OS, 93% versus 95%, $P = 0.310$; EFS, 82% versus 90%, $P = 0.160$) (Table 2).

For comparison with this parameter, we analyzed the survival curves according to the IPI in both treatment groups. The EFS and OS rates at 2 years were 35% and 59% for high or high-intermediate IPI and 77% and 91% for low or low-intermediate IPI, respectively, in the CHOP group. The differences in both EFS and OS rates between the two IPI groups were significant (both $P < 0.001$). Similarly, the EFS and OS rates

were 58% and 80% for high or high-intermediate IPI and 86% and 94% for low or low-intermediate IPI, respectively, in the RCHOP group. Again, the differences in the EFS and OS rates were significant ($P < 0.001$ and $P = 0.004$, respectively).

To estimate unbiased prognostic impacts, Cox univariate analysis showed that a high SIL-2R level, high PS, advanced stage, multiple extranodal sites and high or high-intermediate risk of IPI were associated with poor EFS and OS in both treatment groups (Table 3). In the second step, Cox multivariate analysis showed that only SIL-2R was significantly associated with a higher risk of event and that SIL-2R and PS were independently associated with poor OS in both treatment groups (Table 4). Finally, SIL-2R was a significant risk factor for EFS and a borderline risk factor for OS in both the CHOP and RCHOP groups ($P = 0.060$ and 0.070, respectively), whereas IPI was a significant risk factor for EFS and OS in the CHOP group and a borderline significant risk factor for EFS and OS ($P = 0.070$ and 0.080, respectively) in the RCHOP group (Table 5).

## discussion

Although SIL-2R is easy to measure, its prognostic value has been underestimated due to its evaluation in smaller populations than those for other parameters, such as IPI [2]. The SIL-2R level was reported to be significantly high in highly aggressive lymphomas [6] and subsequently was recognized to reflect tumor burden and poor outcome [3–8]. However, these
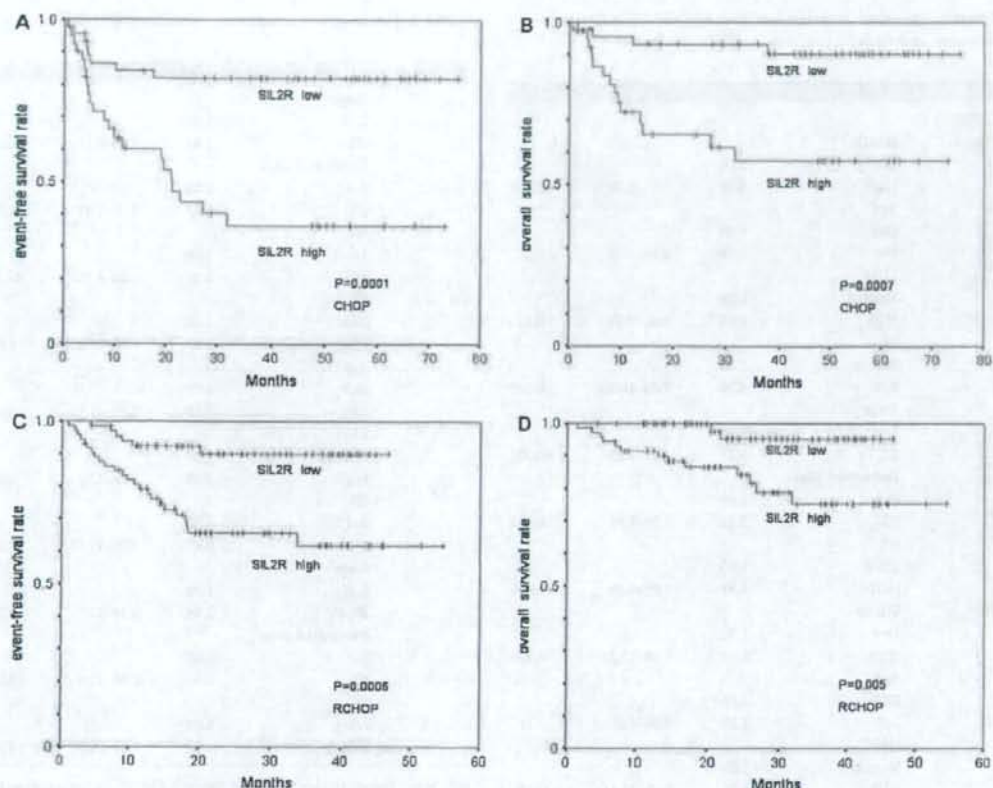
**Figure 1.** Event-free survival (EFS) and overall survival (OS) curves for diffuse large B-cell lymphoma patients treated with cyclophosphamide, doxorubicin, vincristine and prednisone (CHOP) and rituximab-combined CHOP (RCHOP) in relation to soluble interleukin-2 receptor (SIL-2R). EFS (A) and OS (B) curves according to low ($n = 47$) versus high ($n = 40$) SIL-2R in the CHOP group. EFS (C) and OS (D) curves according to low ($n = 67$) versus high ($n = 74$) SIL-2R in the RCHOP group.

**Table 2.** Analysis of 2-year survival rate according to CHOP and RCHOP therapy in both SIL-2R groups

| Clinical outcome | Low SIL-2R | | | High SIL-2R | | |
|---|---|---|---|---|---|---|
| | CHOP | RCHOP | P | CHOP | RCHOP | P |
| 2-year survival | | | | | | |
| EFS (%) | 82 | 90 | 0.160 | 43 | 66 | 0.0010 |
| OS (%) | 93 | 95 | 0.310 | 65 | 84 | 0.0020 |

CHOP, cyclophosphamide, doxorubicin, vincristine and prednisone; RCHOP, rituximab-combined CHOP; SIL2R, soluble interleukin-2 receptor; EFS, event-free survival; OS, overall survival.

results were obtained in patients receiving chemotherapy, and the prognostic value of SIL-2R has not been assessed in rituximab-combined treatment.

In the present study, univariate analysis showed that SIL-2R retained its prognostic value in DLBCL patients treated with RCHOP, as well as in those receiving CHOP alone. Multivariate analysis also showed that SIL-2R was an independent significant prognostic factor after adjustment for IPI risk factors and independently associated with significantly decreased EFS and moderately decreased OS after adjustment by two-categorized IPI in both the CHOP and RCHOP groups. On the other hand, the clinical outcome of patients with high SIL-2R was significantly improved by addition of rituximab to the chemotherapy, in contrast to the lack of any difference in the patients with low SIL-2R. To our knowledge, this is the first report to demonstrate the prognostic value of SIL-2R in DLBCL patients treated with rituximab-combined chemotherapy.

Although the present study was not a randomized prospective one, and possibly biased by factors other than IPI and SIL-2R, the distribution of baseline characteristics, including IPI factors, was similar between the two treatment groups. On the other hand, the population employed in the present analysis had more limited disease and a favorable IPI score compared with those in previous studies of DLBCL [13–17]. This might account for the better outcome of our

# original article

**Table 3.** The effects of clinical factors on EFS and OS in CHOP by univariate analysis using Cox proportional hazard model

| | Variable | HR | 95% CI | P value |
|---|---|---|---|---|
| CHOP | | | | |
| EFS | SIL-2R | | | |
| | Low | 1.00 | | |
| | High | 4.30 | 1.94–9.74 | <0.001 |
| | Age | | | |
| | ≤60 | 1.00 | | |
| | >60 | 1.48 | 0.64–3.46 | 0.36 |
| | LDH | | | |
| | Normal | 1.00 | | |
| | High | 2.65 | 0.80–8.74 | 0.11 |
| | PS | | | |
| | 0–1 | 1.00 | | |
| | 2–3 | 4.10 | 1.64–10.25 | 0.003 |
| | Stage | | | |
| | I, II | 1.00 | | |
| | III, IV | 3.75 | 1.79–7.83 | <0.001 |
| | Extranodal sites | | | |
| | 0–1 | 1.00 | | |
| | ≤2 | 3.24 | 1.54–6.81 | 0.002 |
| | IPI | | | |
| | L/L-I | 1.00 | | |
| | H/H-I | 3.97 | 1.91–8.25 | <0.001 |
| OS | SIL-2R | | | |
| | Low | 1.00 | | |
| | High | 5.64 | 1.84–17.23 | 0.002 |
| | Age | | | |
| | ≤60 | 1.00 | | |
| | >60 | 2.20 | 0.64–7.61 | 0.21 |
| | LDH | | | |
| | Normal | 1.00 | | |
| | High | 4.71 | 0.63–35.41 | 0.13 |
| | PS | | | |
| | 0–1 | 1.00 | | |
| | 2–3 | 7.18 | 2.44–21.13 | <0.001 |
| | Stage | | | |
| | I, II | 1.00 | | |
| | III, IV | 5.15 | 1.92–13.81 | 0.001 |
| | Extranodal sites | | | |
| | 0–1 | 1.00 | | |
| | ≤2 | 4.24 | 1.64–10.98 | 0.003 |
| | IPI | | | |
| | L/L-I | 1.00 | | |
| | H/H-I | 7.28 | 2.69–19.67 | <0.001 |
| RCHOP | | | | |
| EFS | SIL-2R | | | |
| | Low | 1.00 | | |
| | High | 4.20 | 1.72–10.33 | 0.002 |
| | Age | | | |
| | ≤60 | 1.00 | | |
| | >60 | 1.38 | 0.61–3.11 | 0.44 |
| | LDH | | | |
| | Normal | 1.00 | | |
| | High | 1.41 | 0.68–2.93 | 0.35 |
| | PS | | | |
| | 0–1 | 1.00 | | |
| | 2–3 | 3.62 | 1.35–8.46 | 0.003 |

**Table 3.** (*Continued*)

| | Variable | HR | 95% CI | P value |
|---|---|---|---|---|
| | Stage | | | |
| | I, II | 1.00 | | |
| | III, IV | 3.42 | 1.64–7.11 | 0.001 |
| | Extranodal sites | | | |
| | 0–1 | 1.00 | | |
| | ≤2 | 3.43 | 1.67–7.03 | <0.001 |
| | IPI | | | |
| | L/L-I | 1.00 | | |
| | H/H-I | 3.40 | 1.82–6.25 | <0.001 |
| OS | SIL-2R | | | |
| | Low | 1.00 | | |
| | High | 6.42 | 1.45–28.45 | 0.01 |
| | Age | | | |
| | ≤60 | 1.00 | | |
| | >60 | 3.50 | 0.79–15.52 | 0.10 |
| | LDH | | | |
| | Normal | 1.00 | | |
| | High | 1.69 | 0.58–4.97 | 0.34 |
| | PS | | | |
| | 0–1 | 1.00 | | |
| | 2–3 | 5.97 | 2.03–17.54 | 0.001 |
| | Stage | | | |
| | I, II | 1.00 | | |
| | III, IV | 2.46 | 0.89–6.79 | 0.08 |
| | Extranodal sites | | | |
| | 0–1 | 1.00 | | |
| | ≤2 | 2.65 | 0.96–7.33 | 0.06 |
| | IPI | | | |
| | L/L-I | 1.00 | | |
| | H/H-I | 4.03 | 1.43–11.34 | 0.08 |

EFS, event-free survival; OS, overall survival; CHOP, cyclophosphamide, doxorubicin, vincristine and prednisone; RCHOP, rituximab-combined CHOP; HR, hazard ratio; CI, confidential interval; SIL2R, soluble interleukin-2 receptor; LDH, lactate dehydrogenase; PS, performance status; IPI, International Prognostic Index; L/L-I, low or low-intermediate; H/H-I, high or high-intermediate.

patients than for those in previous reports such as that by Coiffier et al. [14] who observed 2-year survival rates of 70% and 57% in elderly patients treated with RCHOP and CHOP, respectively. Even with the excellent outcome we observed, however, the prognostic value of SIL-2R was significant and greater than that of other IPI risk factors. To allow our present results to be generalized to routine patient care, these findings should be validated in a variety of patient populations.

A number of prognostic markers have been identified in patients with DLBCL treated by chemotherapy alone [19–21], some of which have been reassessed and shown not to be associated with prognosis in patients receiving rituximab-combined chemotherapy [22–24]. BCL2 overexpression was reported to be associated with poorer survival in patients treated with CHOP-like regimens [19], but its prognostic value was not confirmed in patients receiving rituximab-combined chemotherapy in several studies, indicating that addition of rituximab overcomes the negative influence of BCL2

**Table 4.** Multivariate Cox proportional hazard regression analysis for
SIL-2R and IPI risk factors in both treatment groups

| | Variable | HR | 95% CI | P value |
|---|---|---|---|---|
| CHOP | | | | |
| EFS | SIL-2R | | | |
| | Low | 1.00 | | |
| | High | 2.74 | 1.05–7.14 | 0.04 |
| | PS | | | |
| | 0–1 | 1.00 | | |
| | 2–3 | 2.12 | 0.73–6.14 | 0.17 |
| | Stage | | | |
| | I, II | 1.00 | | |
| | III, IV | 1.82 | 0.65–5.09 | 0.25 |
| | Extranodal sites | | | |
| | 0–1 | 1.00 | | |
| | ≤2 | 1.09 | 0.38–3.10 | 0.87 |
| OS | SIL-2R | | | |
| | Low | 1.00 | | |
| | High | 3.53 | 1.03–12.95 | 0.05 |
| | LDH | | | |
| | Normal | 1.00 | | |
| | High | 3.21 | 0.40–25.51 | 0.27 |
| | PS | | | |
| | 0–1 | 1.00 | | |
| | 2–3 | 3.60 | 0.98–13.20 | 0.05 |
| | Stage | | | |
| | I, II | 1.00 | | |
| | III, IV | 2.00 | 0.51–7.87 | 0.32 |
| | Extranodal sites | | | |
| | 0–1 | 1.00 | | |
| | ≤2 | 0.86 | 0.22–0.83 | 0.83 |
| RCHOP | | | | |
| EFS | SIL-2R | | | |
| | Low | 1.00 | | |
| | High | 2.65 | 1.01–7.30 | 0.05 |
| | PS | | | |
| | 0–1 | 1.00 | | |
| | 2–3 | 1.66 | 0.62–4.42 | 0.31 |
| | Stage | | | |
| | I, II | 1.00 | | |
| | III, IV | 1.69 | 0.65–4.42 | 0.28 |
| | Extranodal sites | | | |
| | 0–1 | 1.00 | | |
| | ≤2 | 1.36 | 0.50–3.67 | 0.55 |
| OS | SIL-2R | | | |
| | Low | 1.00 | | |
| | High | 5.09 | 1.00–25.88 | 0.05 |
| | Age | | | |
| | ≤60 | 1.00 | | |
| | >60 | 2.45 | 0.54–11.17 | 0.24 |
| | PS | | | |
| | 0–1 | 1.00 | | |
| | 2–3 | 4.49 | 1.15–17.45 | 0.03 |
| | Stage | | | |
| | I, II | 1.00 | | |
| | III, IV | 1.02 | 0.23–4.45 | 0.98 |
| | Extranodal sites | | | |
| | 0–1 | 1.00 | | |
| | ≤2 | 0.70 | 0.15–3.39 | 0.66 |

SIL2R, soluble interleukin-2 receptor; IPI, International Prognostic Index;
CHOP, cyclophosphamide, doxorubicin, vincristine and prednisone; HR,
hazard ratio; CI, confidential interval; EFS, event-free survival; PS,
performance status; OS, overall survival; LDH, lactate dehydrogenase;
RCHOP, rituximab-combined CHOP.

**Table 5.** Multivariate Cox proportional hazard analysis for SIL-2R and
categorized IPI in both treatment groups

| | Variable | HR | 95% CI | P value |
|---|---|---|---|---|
| CHOP | | | | |
| EFS | SIL-2R | | | |
| | Low | 1.00 | | |
| | High | 2.98 | 1.22–7.29 | 0.01 |
| | IPI | | | |
| | L/L-I | 1.00 | | |
| | H/H-I | 2.47 | 1.11–5.47 | 0.02 |
| OS | SIL-2R | | | |
| | Low | 1.00 | | |
| | High | 3.12 | 0.93–10.41 | 0.06 |
| | IPI | | | |
| | L/L-I | 1.00 | | |
| | H/H-I | 4.66 | 1.60–13.58 | 0.005 |
| RCHOP | | | | |
| EFS | SIL-2R | | | |
| | Low | 1.00 | | |
| | High | 3.00 | 1.12–8.07 | 0.02 |
| | IPI | | | |
| | L/L-I | 1.00 | | |
| | H/H-I | 2.06 | 0.93–4.57 | 0.07 |
| OS | SIL-2R | | | |
| | Low | 1.00 | | |
| | High | 4.30 | 0.85–21.91 | 0.07 |
| | IPI | | | |
| | L/L-I | 1.00 | | |
| | H/H-I | 4.16 | 0.80–6.69 | 0.08 |

SIL2R, soluble interleukin-2 receptor; IPI, International Prognostic Index;
CHOP, cyclophosphamide, doxorubicin, vincristine and prednisone; HR,
hazard ratio; CI, confidential interval; EFS, event-free survival; OS, overall
survival; LDH, lactate dehydrogenase; RCHOP, rituximab-combined
CHOP; L/L-I, low or low-intermediate; H/H-I, high or high-intermediate.

overexpression [24]. BCL6, a marker of germinal center
derivation, has been identified as an indicator of favorable
outcome in DLBCL [20], although outcome in patients
receiving immunochemotherapy was reported to be
uninfluenced by BCL6 status [22]. Similarly, no correlation
between immunohistochemically defined GC phenotype and
survival rate was observed in patients receiving
immunochemotherapy [21], in contrast to previous findings
of inferior outcomes in non-GC patients relative to GC patients
in the prerituximab era [23]. Up to now, no marker other than
IPI has been found to be of prognostic relevance since the
clinical introduction of rituximab.

The mechanism by which rituximab added to chemotherapy
improves outcome in relation to biological features has been
evaluated in several studies. They showed that rituximab may
suppress the constitutively active nuclear factor-kappa B
pathway in non-GC phenotype DLBCL or downregulate Bcl-2-
related antiapoptotic proteins, thereby increasing the sensitivity
of lymphoma cells to chemotherapy [27–29]. These effects of
rituximab may reduce the prognostic significance of the non-
GC phenotype and BCL2. Although the mechanism by which
SIL-2R retains its prognostic value after addition of rituximab
to chemotherapy is unknown, SIL-2R may directly represent
the tumor burden [7, 8].